Mean-field based approach for collective excitations in neutron-rich nuclei

Kenichi Yoshida
Kyoto Univ.

Frontier explored by RIBF

15 years since the full-scale operation started

187 new isotopes discovered at RIKEN

- 32: pre-RIBF
- 50: 2007–2010
- 105: 2011–2021

cf. The last YKIS was held in 2011.

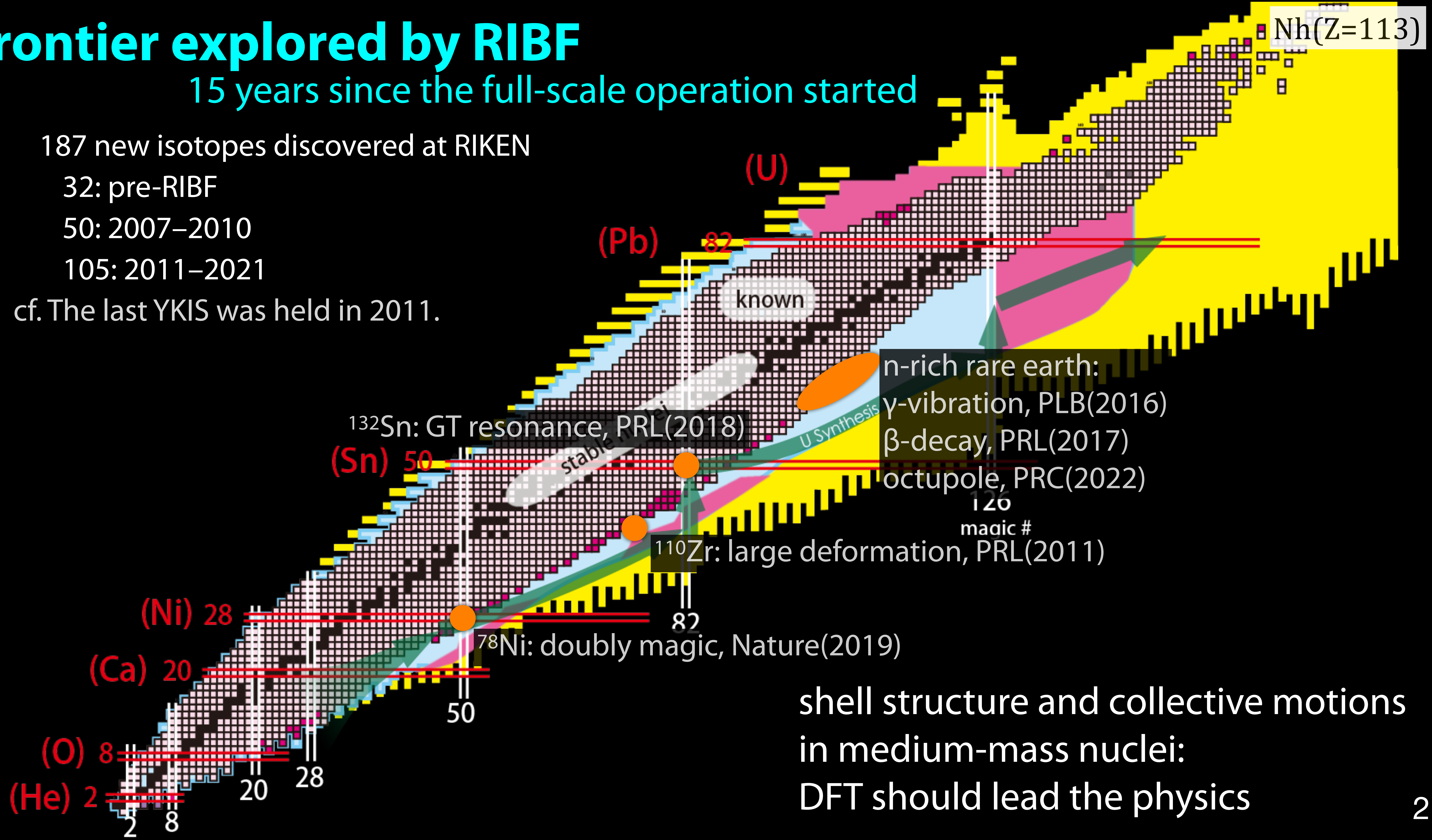

shell structure and collective motions in medium-mass nuclei:
DFT should lead the physics

Nuclear density functional theory (DFT)

Nuclear EDF $E[\rho, \tilde{\rho}, \tilde{\rho}^*]$: Skyrme, Gogny, covariant,…

Kohn–Sham–Bogoliubov–de Gennes (or HFB) method

for the equilibrium configuration

Bulgac(1980), Dobaczewski+(1984)
Oliveira+(1988)

$$\delta(E[\rho, \tilde{\rho}, \tilde{\rho}^*] - \sum_q \lambda^q \langle \hat{N}_q \rangle) = 0$$

$$(\mathscr{H}^q_{\mathrm{HFB}} - \lambda^q \mathscr{N})\Phi^q_\alpha(x) = E^q_\alpha \Phi^q_\alpha(x)$$

$$\mathscr{H}^q_{\mathrm{HFB}}[\rho, \tilde{\rho}, \tilde{\rho}^*] = \sum_{\sigma'} \begin{bmatrix} h^q_{\sigma\sigma'}(\boldsymbol{r}) & \tilde{h}^q_{\sigma\sigma'}(\boldsymbol{r}) \\ 4\sigma\sigma' \tilde{h}^{q*}_{-\sigma-\sigma'}(\boldsymbol{r}) & -4\sigma\sigma' h^{q*}_{-\sigma-\sigma'}(\boldsymbol{r}) \end{bmatrix}, \quad \mathscr{N} = \begin{bmatrix} 1 & 0 \\ 0 & -1 \end{bmatrix} \qquad h = \frac{\delta E}{\delta \rho}, \quad \tilde{h} = \frac{\delta E}{\delta \tilde{\rho}^*}$$

appropriate framework for describing neutron-rich nuclei

asymptotic behavior of densities at large distances

pairing involving the continuum states

Nuclear DFT for equilibrium deformed shapes

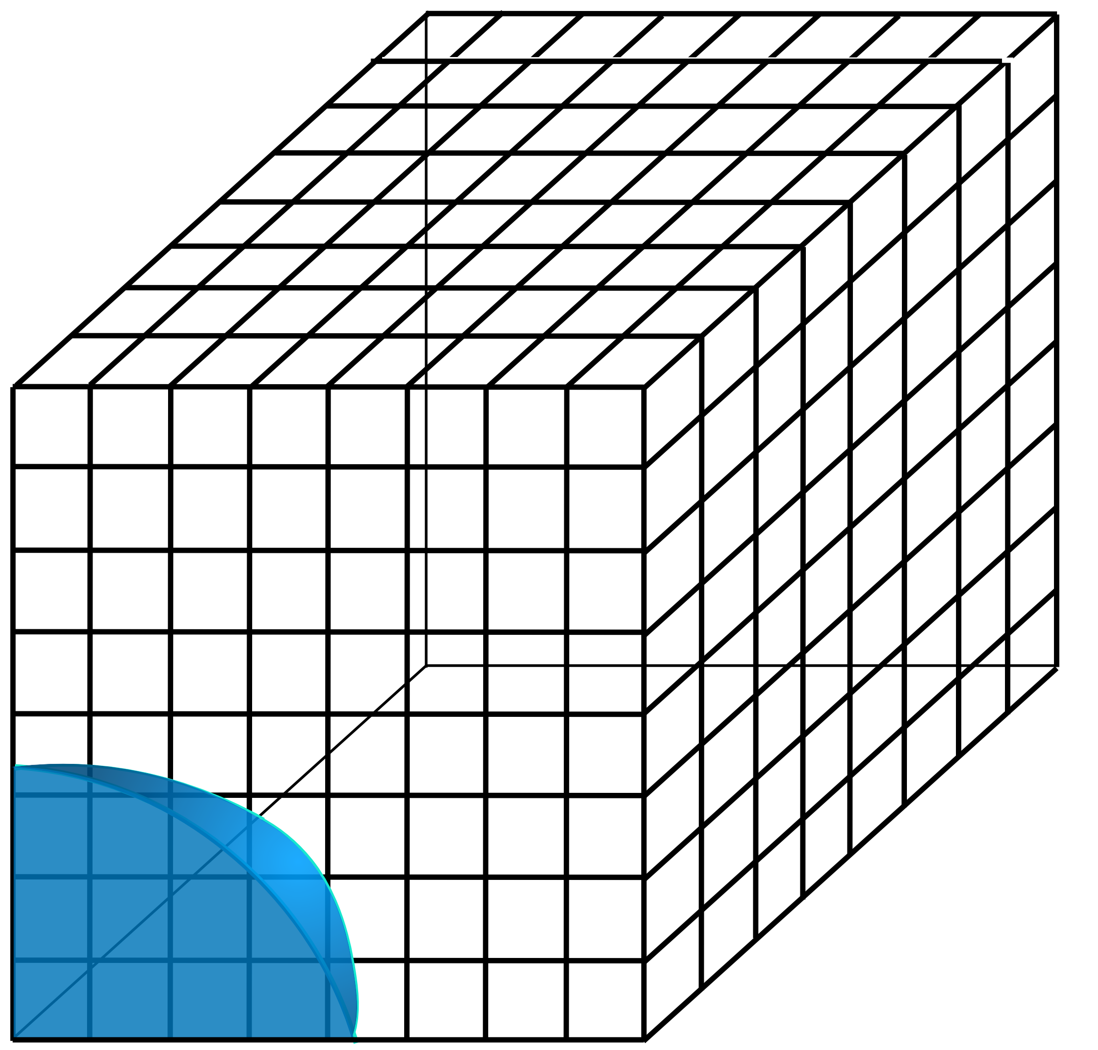

3D-mesh calculation is now available

- Krylov subspace method for the Greens func.
  - Seattle–Warsaw (Jin–Bulgac–Roche–Wlazłowski, 2017)
  - Tsukuba (Kashiwaba–Nakatsukasa, 2020)
- canonical basis and FFT — East Lansing–Erlangen (Chen+, 2022)
- direct diagonalization — KY, 2022

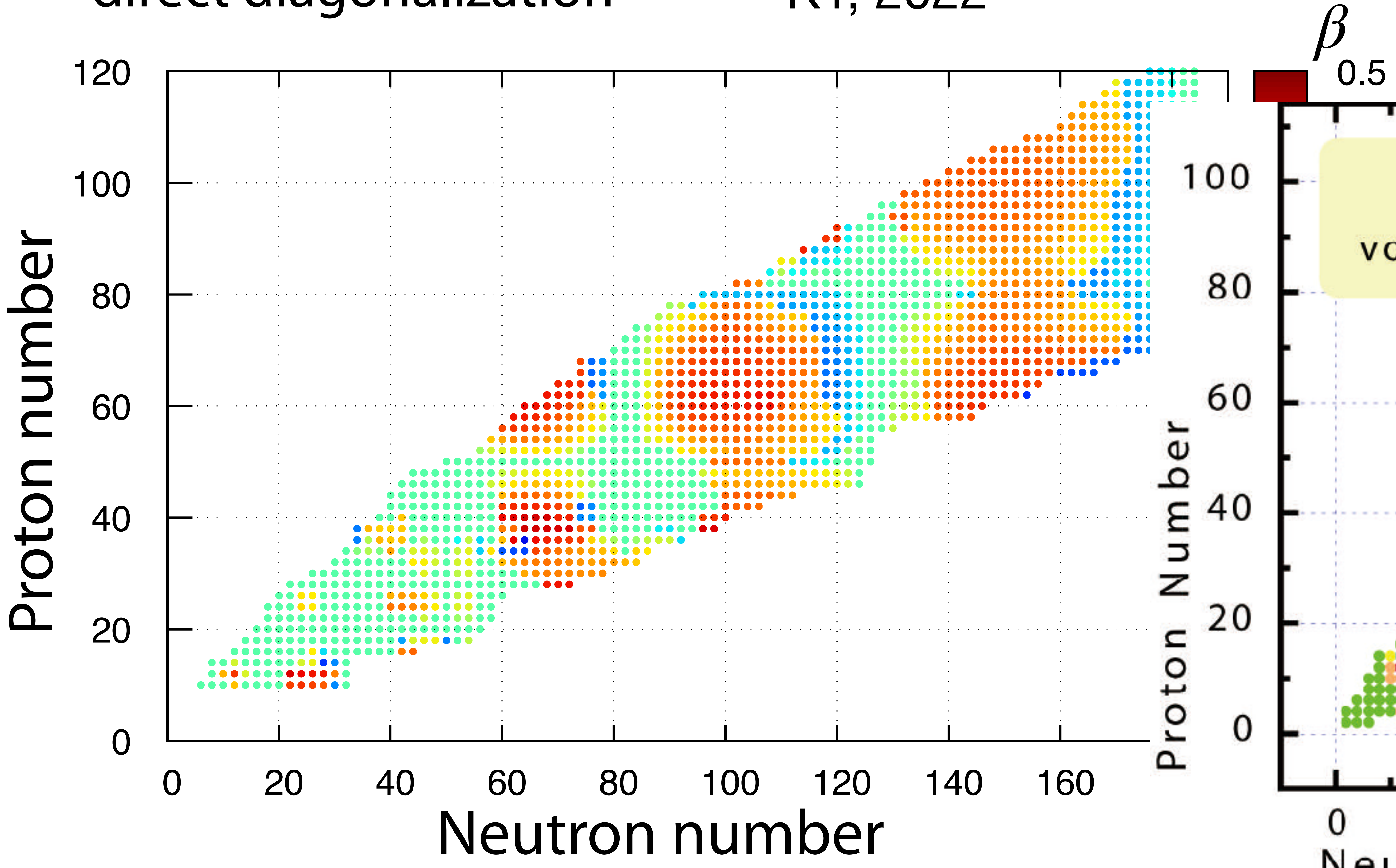

Stoitsov+(2003)

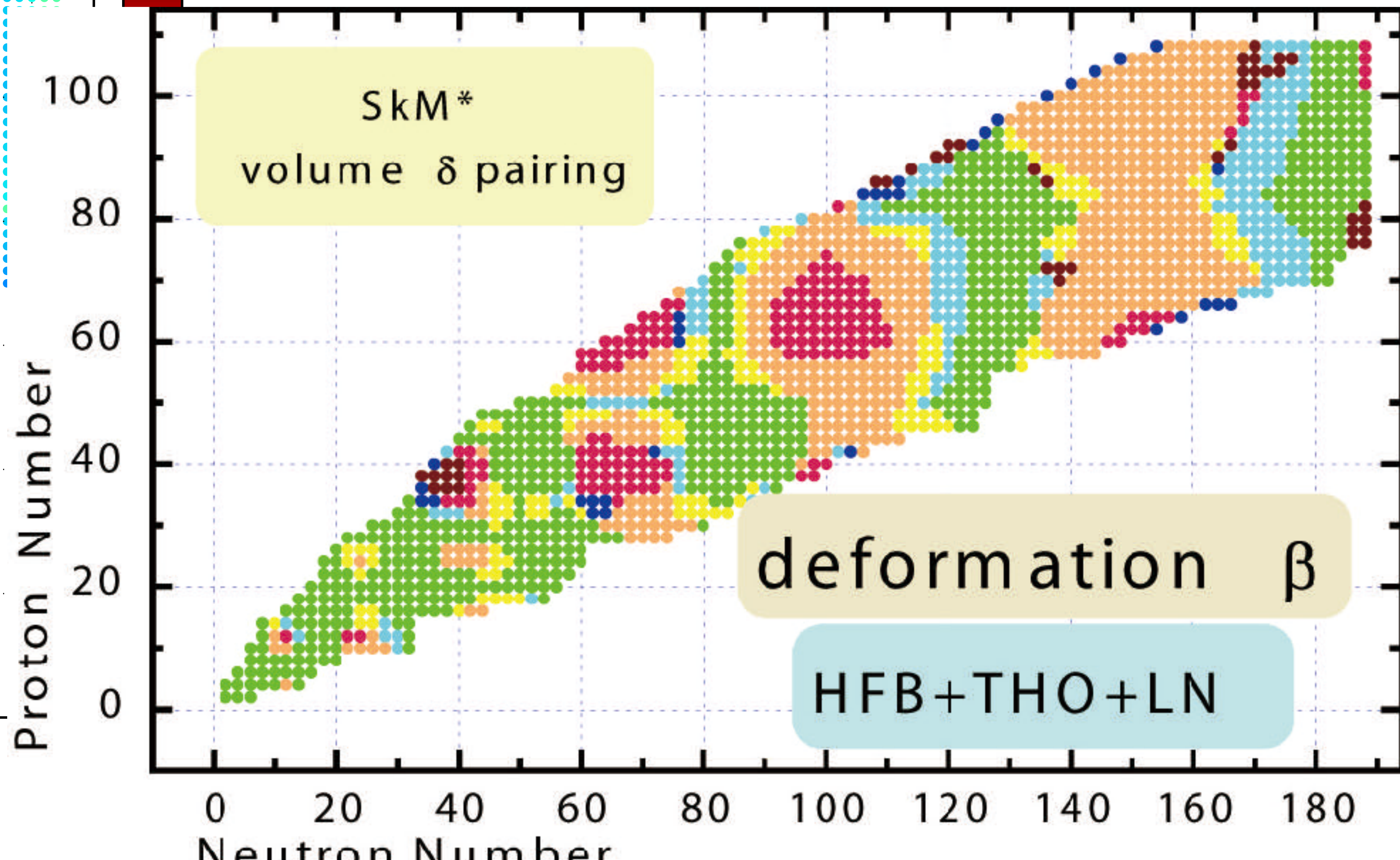

Nuclear DFT for equilibrium deformed shapes

3D-mesh calculation is now available

- Krylov subspace method for the Greens func.
  - Seattle–Warsaw (Jin–Bulgac–Roche–Wlazłowski, 2017)
  - Tsukuba (Kashiwaba–Nakatsukasa, 2020)
- canonical basis and FFT   East Lansing–Erlangen (Chen+, 2022)
- direct diagonalization   KY, 2022

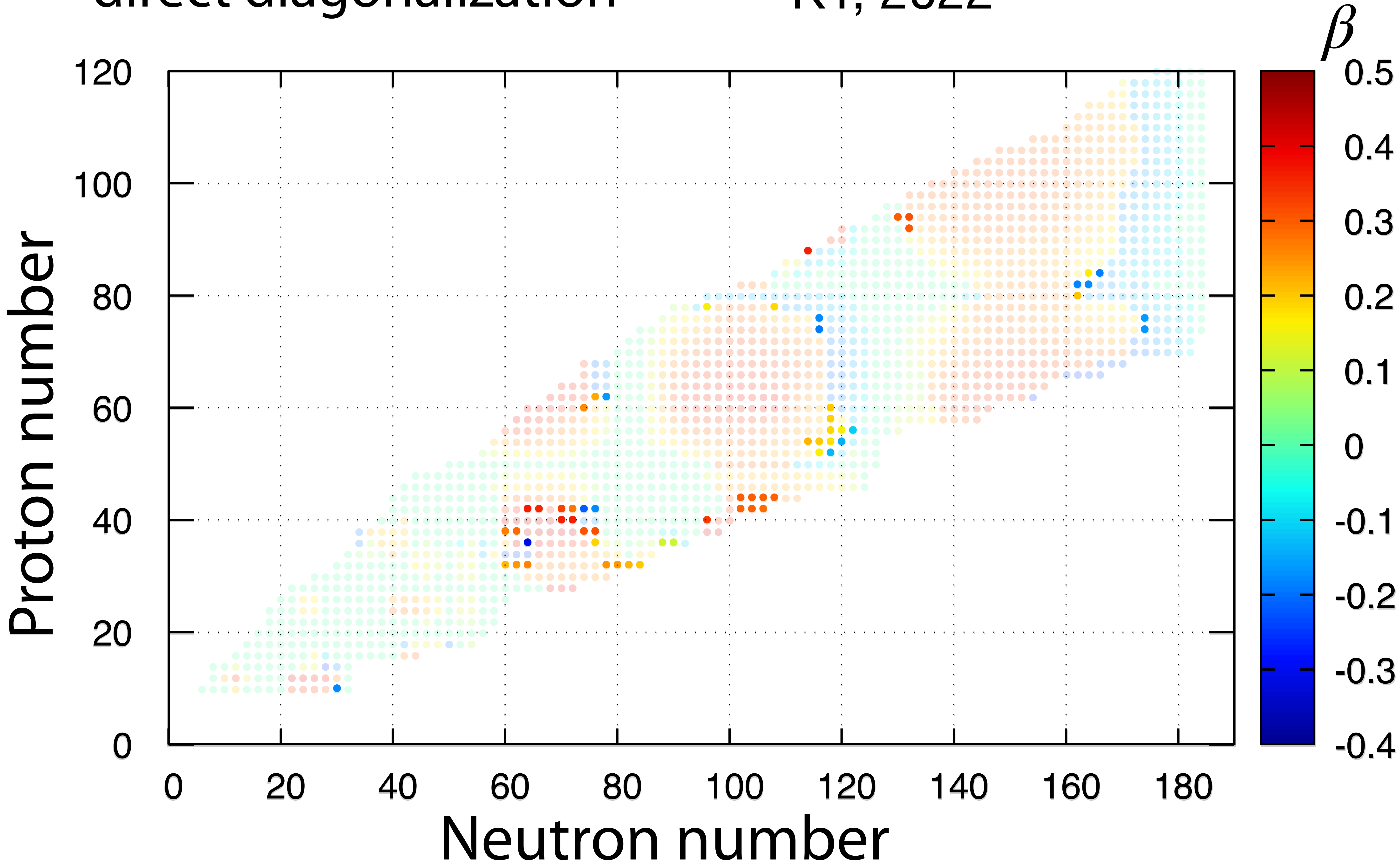

triaxial deformation

$10^\circ < \gamma < 50^\circ$

triaxially-deformed drip-line nuclei

Triaxiality-induced halo structure

Uzawa–Hagino–Yoshida (2021)

condition for the halo

spherical: $\ell = 0{,}1$ only

axially-def.: $\Omega^\pi = 1/2^\pm, 3/2^-$ only

triaxially-def.: any Ω^π

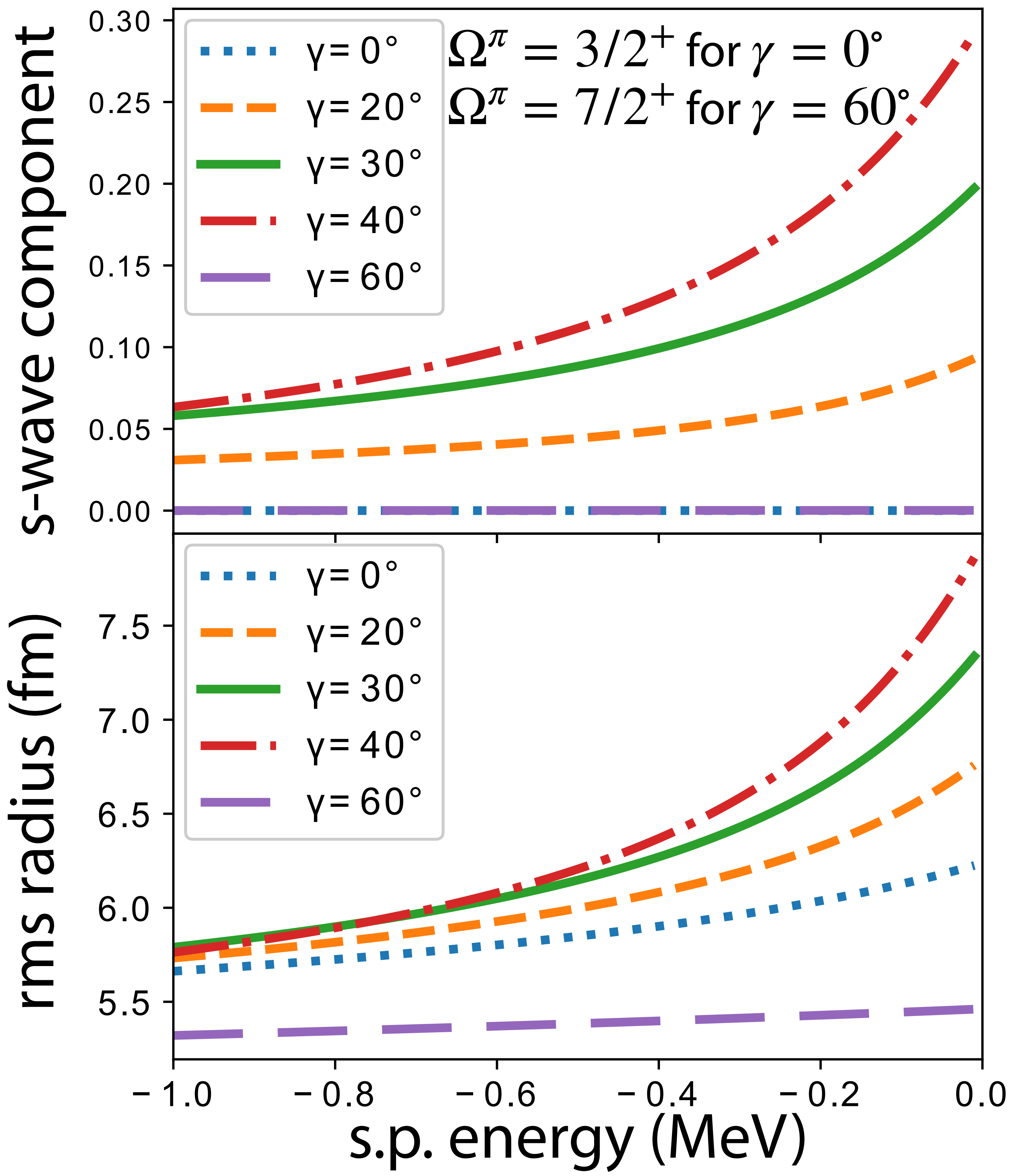

near the drip line

symmetries broken as much as possible to obtain a deeper binding

releasing the kinetic energy → halo

systematic 3D-mesh cal. with a large box size

Nuclear DFT for collective motions

Time-dependent DFT for dynamics: TD-KSB approach

$$i\partial_t R^q(t) = [\mathscr{H}^q_{\mathrm{HFB}}(t) - \lambda^q \mathscr{N}, R^q(t)] \qquad R = \Phi\Phi^\dagger$$

for collective rotations

$$\Phi'(t) = U\Phi(t) = \exp[i\omega \hat{J}_x \mathscr{N} t]\Phi(t)$$ in a uniformly rotating system about x-axis

$$i\partial_t R'^q(t) = [\mathscr{H}^q_{\mathrm{HFB}} - (\lambda^q + \omega \hat{J}_x)\mathscr{N}, R'^q(t)]$$

stationary

cranked KSB equation

$$[\mathscr{H}^q_{\mathrm{HFB}} - (\lambda^q + \omega \hat{J}_x)\mathscr{N}]\Phi'^q_\alpha(x) = E'^q_\alpha \Phi'^q_\alpha(x)$$

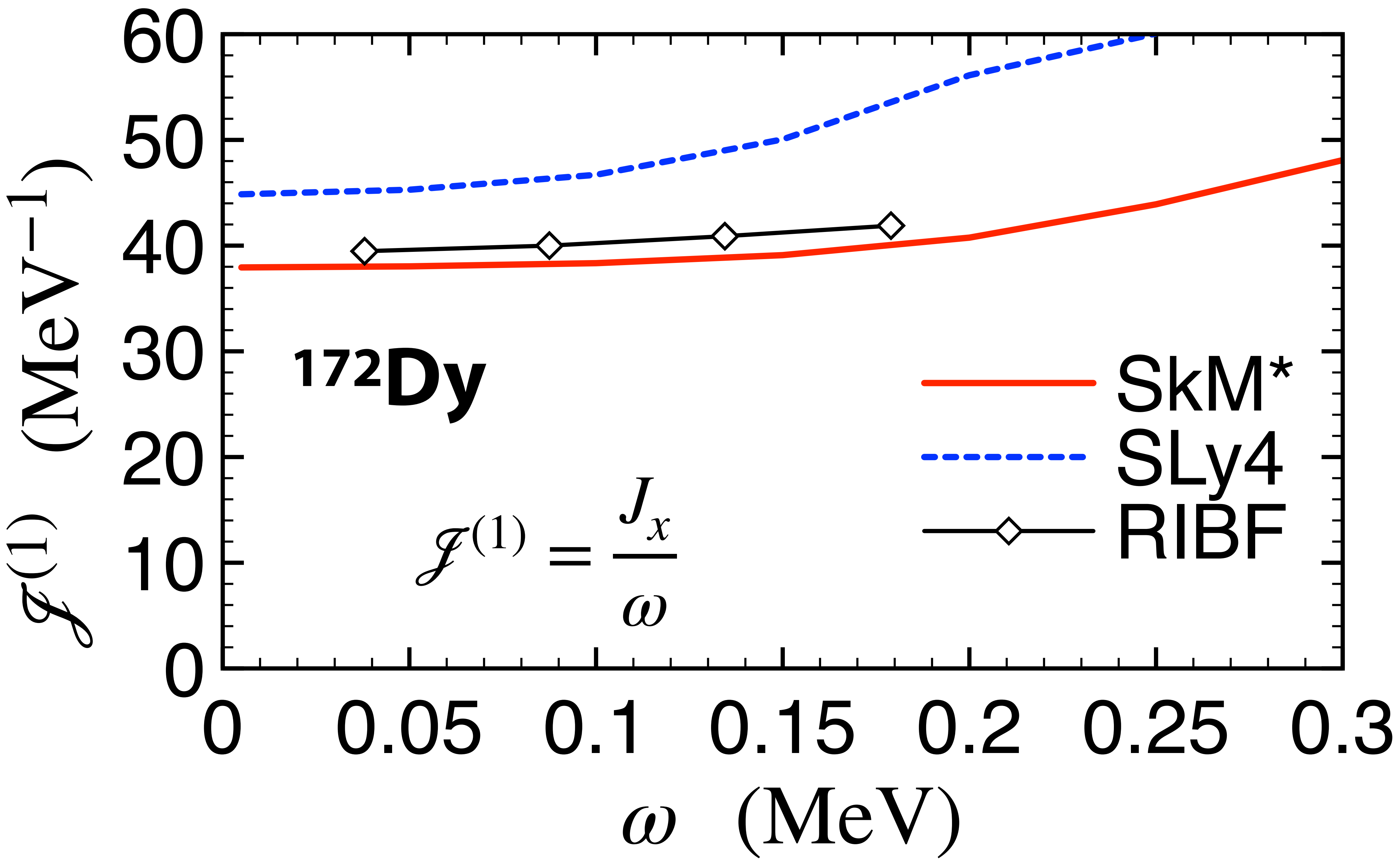

Validity of the cranking model for the 2_1^+ state energy

KY, arXiv:2205.01814

Exp.:

657 even-even nuclei with known $E(2_1^+)$ in NNDC

22 nuclei with $Z < 10$; Skyrme EDF is least justified

Cranking model: $E(2^+) = \dfrac{3}{\mathscr{J}}$, $\mathscr{J} = \lim_{\omega\to 0} \dfrac{J_x}{\omega}$ evaluated at $\omega = 0.05$ MeV

no rotation in spherical nuclei: 273 (260) nuclei with SkM* (SLy4)

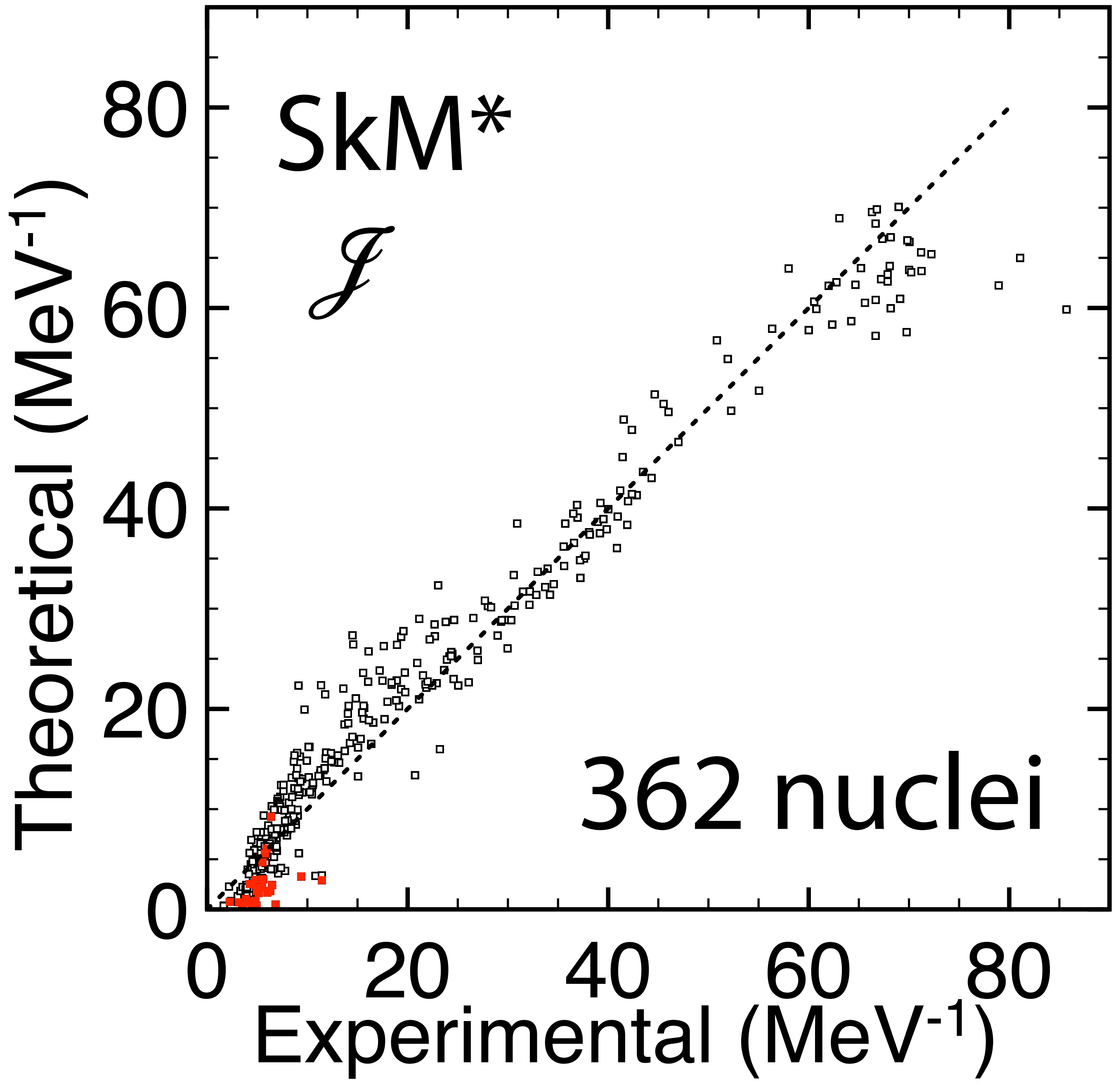

$R = \mathscr{J}_{\rm th}/\mathscr{J}_{\rm exp}$

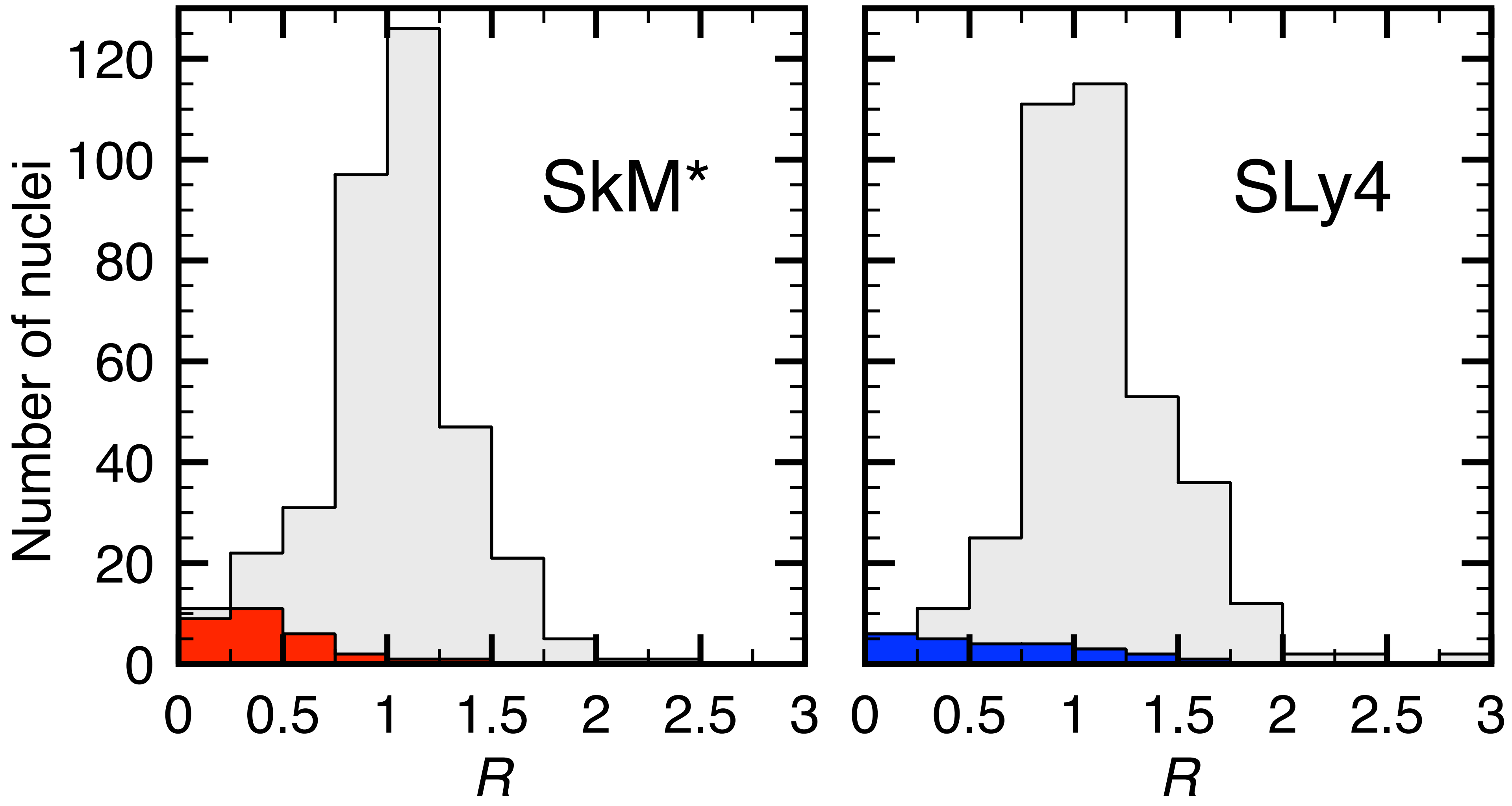

Validity of the cranking model for the 2_1^+ state energy

KY, arXiv:2205.01814

model	# of nuclei	$\bar{R}_E$	σ_E
CHFB(SkM*)	332	-0.021	0.33
CHFB(SLy4)	335	-0.095	0.30
MAP(SL4)	359	0.28	0.49
MAP(SLy4,def)	135	0.20	0.30
GCM(SLy4)	359	0.51	0.38
GCM(SLy4,def)	135	0.27	0.33
5DCH(D1S)	519	0.12	0.33
5DCH(D1S,def)	146	-0.05	0.19

MAP (minimization after projection), Sabby+(2007)
GCM (Hill–Wheeler), Sabby+(2007)
5DCH (GCM+GOA), Bertsch+(2007)

$$R_E = \ln(E_{\rm th}(2^+)/E_{\rm exp}(2^+))$$

$$\sigma_E = \sqrt{\langle (R_E - \bar{R}_E)^2 \rangle}$$

self-consistent cranking model surprisingly well describes $E(2^+)$

$$E \not\sim I(I+1)$$

30–35% error implies a variety of characters of individual nuclides

MoI of neutron-rich nuclei

KY, arXiv:2205.01814

$E(2^+)$: indicator for the evolution of shell structure and deformation

cf. SEASTAR

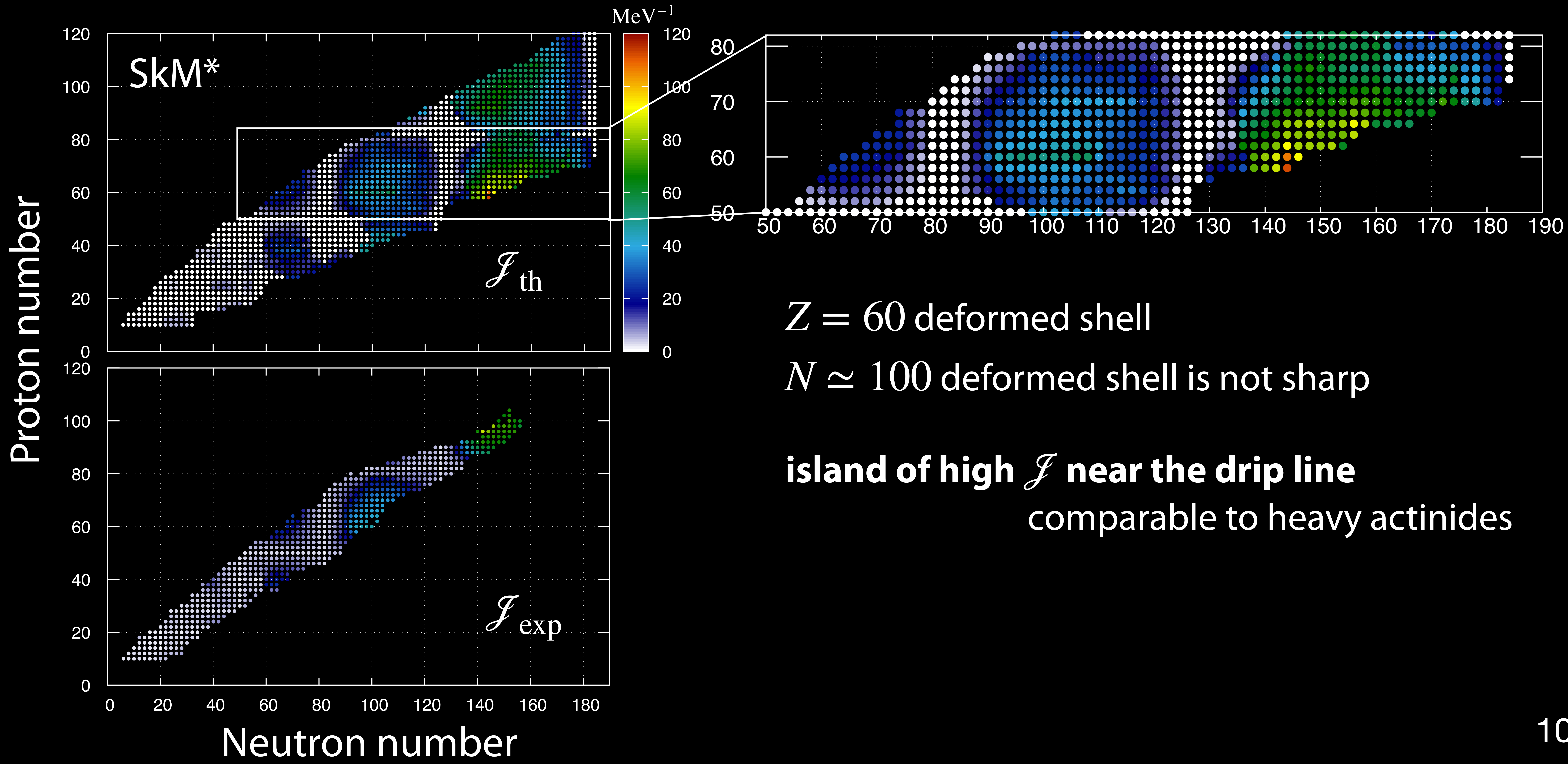

$Z = 60$ deformed shell

$N \simeq 100$ deformed shell is not sharp

island of high $\mathscr{J}$ near the drip line

comparable to heavy actinides

MoI of neutron-rich Dy isotopes

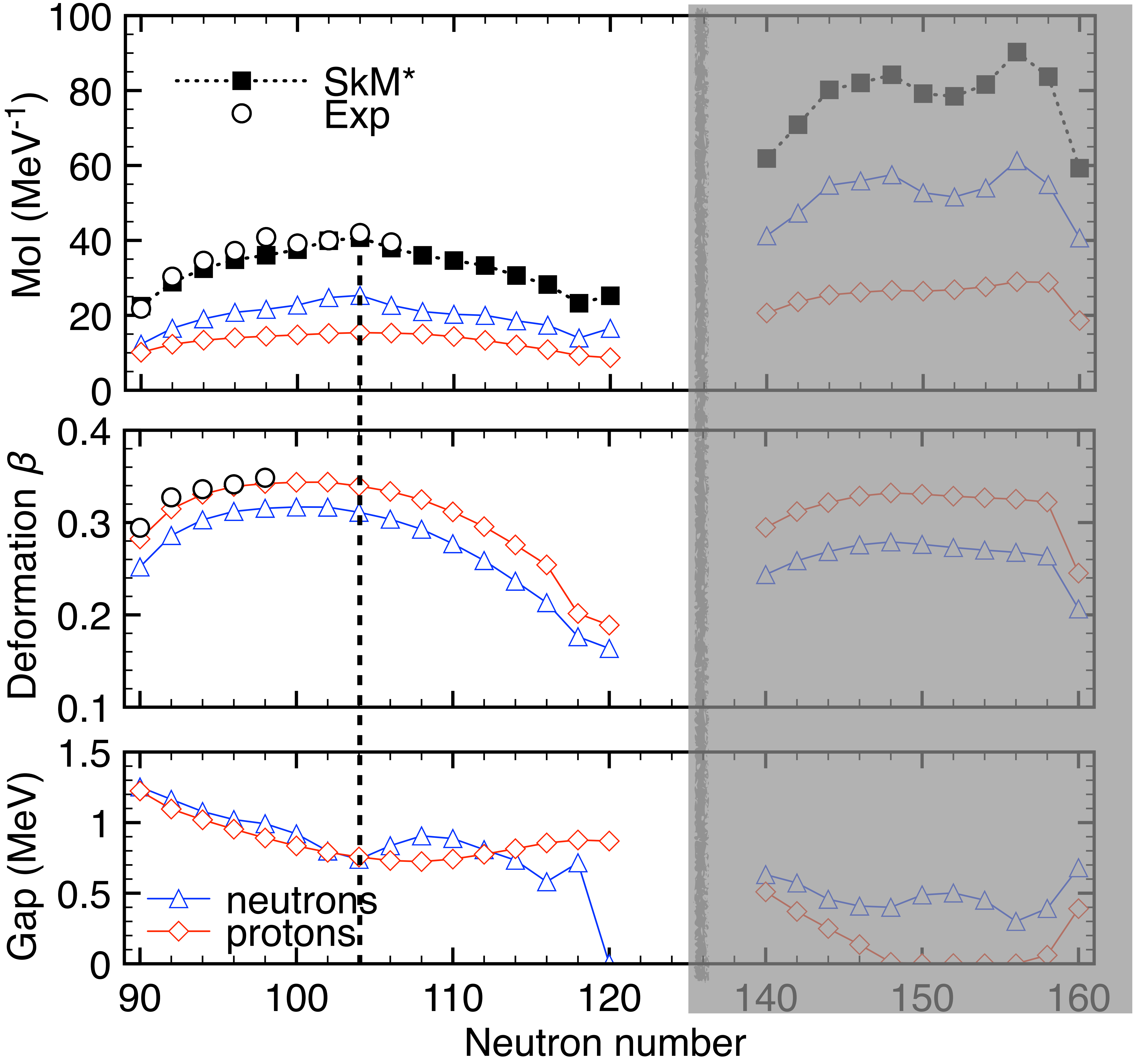

$\mathscr{J}$ is highest at $N = 104$

both in exp. and cal.

Δ_n is lowest at $N = 104$

deformation develops toward $N = 100$

$\mathscr{J} \leftrightarrow \beta$ is not a one-to-one correspondence

$E(2^+) \leftrightarrow B(E2)$

$\mathscr{J}$ is much more sensitive to the shell structure and pairing

MoI of neutron-rich Dy isotopes: A role of the pairing

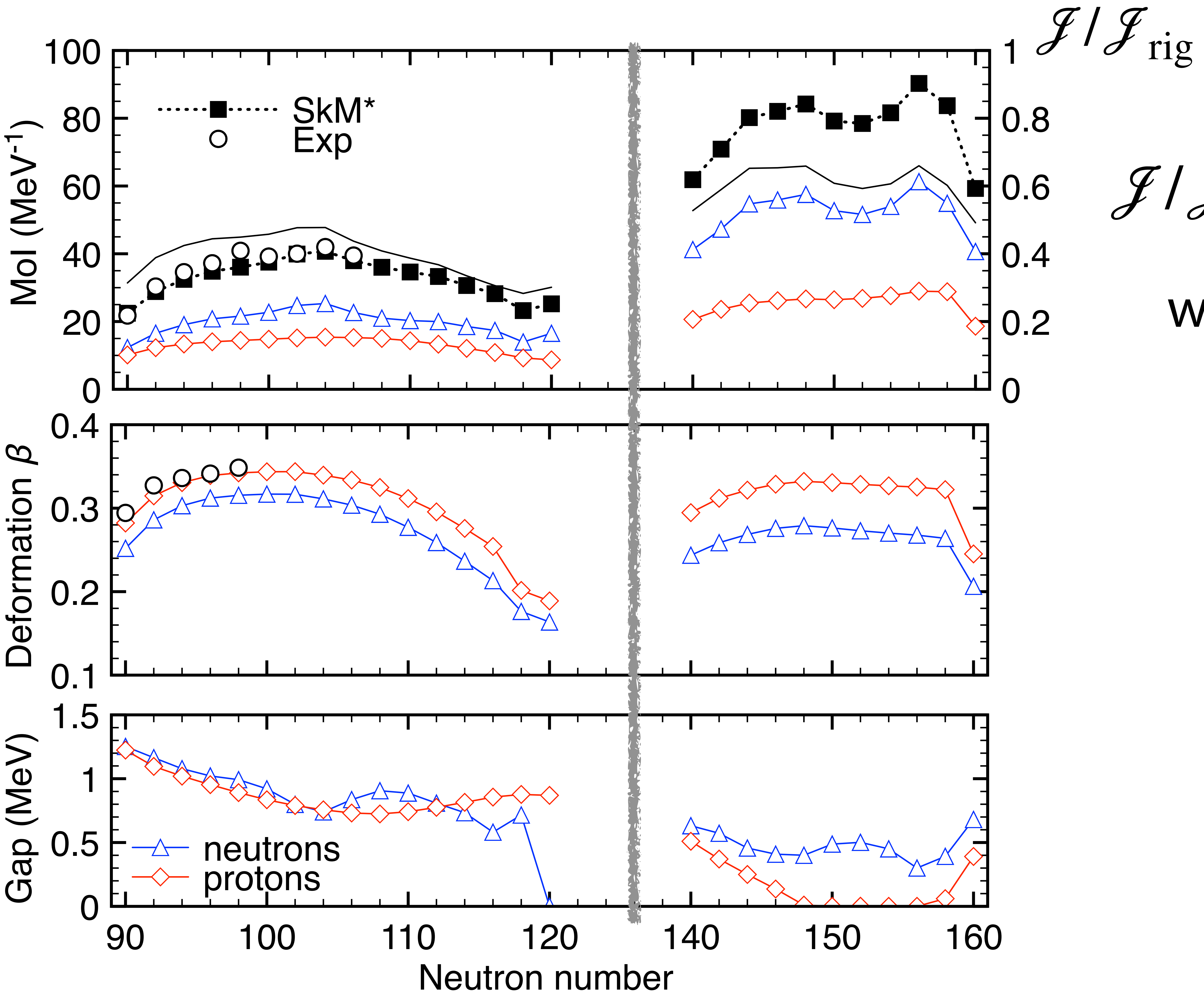

$\mathscr{J}/\mathscr{J}_{\rm rig}$ is higher in $N \simeq 150$

weakening of the pairing

high isovector density in n-rich

$$\mathscr{E}_{\rm pair}(\boldsymbol{r}) = \frac{V_0}{4}\sum_{\tau={\rm n,p}} g_\tau[\rho,\rho_1]\,|\tilde{\rho}_\tau(\boldsymbol{r})|^2$$

$$g_\tau[\rho,\rho_1] = 1 - \eta_0\frac{\rho(\boldsymbol{r})}{\rho_0} - \eta_1\frac{\tau_3\rho_1(\boldsymbol{r})}{\rho_0} - \eta_2\left[\frac{\rho_1(\boldsymbol{r})}{\rho_0}\right]^2$$

$$\eta_1, \eta_2 > 0$$

Yamagami–Shimizu–Nakatsukasa ('09)

Nuclear DFT for collective motions: vibrations

Time-dependent DFT $\rho(\mathbf{r},t) = \rho_0(\mathbf{r}) + \delta\rho(\mathbf{r},t) + \mathrm{h.c.}$

linear response to the external field: $e^{-i\omega t}\hat{F} = e^{-i\omega t}\int d\mathbf{r} f(\mathbf{r})\hat{\psi}^\dagger(\mathbf{r})\hat{\psi}(\mathbf{r})$

$\delta\rho(\mathbf{r},t) \sim \delta\rho(\mathbf{r})e^{-i\omega t}$ $\quad\quad$ $\delta\rho(\mathbf{r}) = \int d\mathbf{r}'\chi_0(\mathbf{r},\mathbf{r}')\left[\frac{\delta^2 E[\rho]}{\delta^2\rho}\delta\rho(\mathbf{r}') + f(\mathbf{r}')\right]$

vibration in space/spin-space/isospin-space/gauge-space and couping among them

$$\hat{F}_L = \int dr \sum_{\sigma\sigma'}\sum_{\tau\tau'} r^L Y_L(\hat{r}) O(\sigma\tau,\sigma'\tau')\hat{\psi}^\dagger(\boldsymbol{r}\sigma\tau)\hat{\psi}(\boldsymbol{r}\sigma'\tau') \text{ or } \hat{\psi}^\dagger(\boldsymbol{r}\sigma\tau)\hat{\psi}^\dagger(\boldsymbol{r}\tilde{\sigma}'\tilde{\tau}')$$

rich variety of modes of vibration

^{172}Dy: heaviest n-rich nucleus with spectroscopic info

Watanabe+, PLB760(2016)641

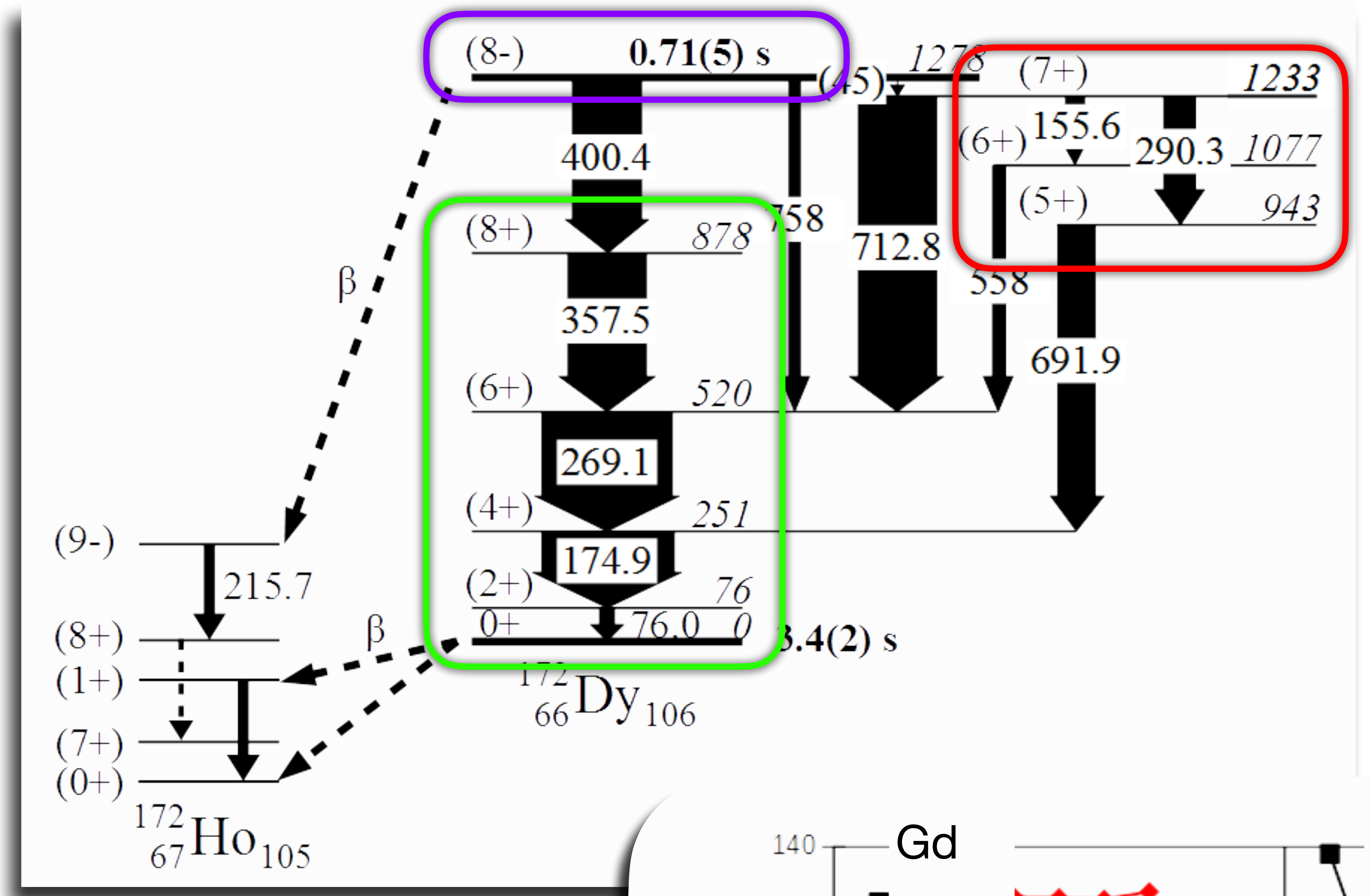

Long-lived isomeric state

Ground-state rotational band

Possible gamma band

Decrease in the excitation energy at *N*=106

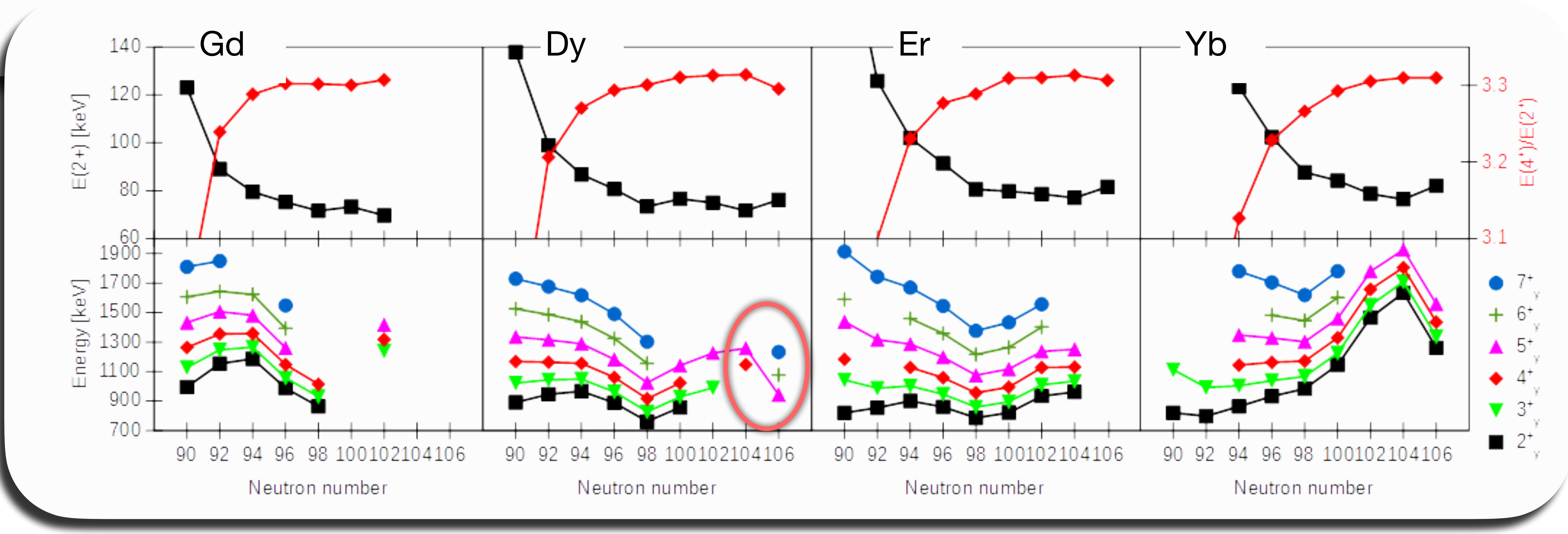

Gamma vibration in n-rich Dy isotopes

Yoshida–Watanabe (2016)

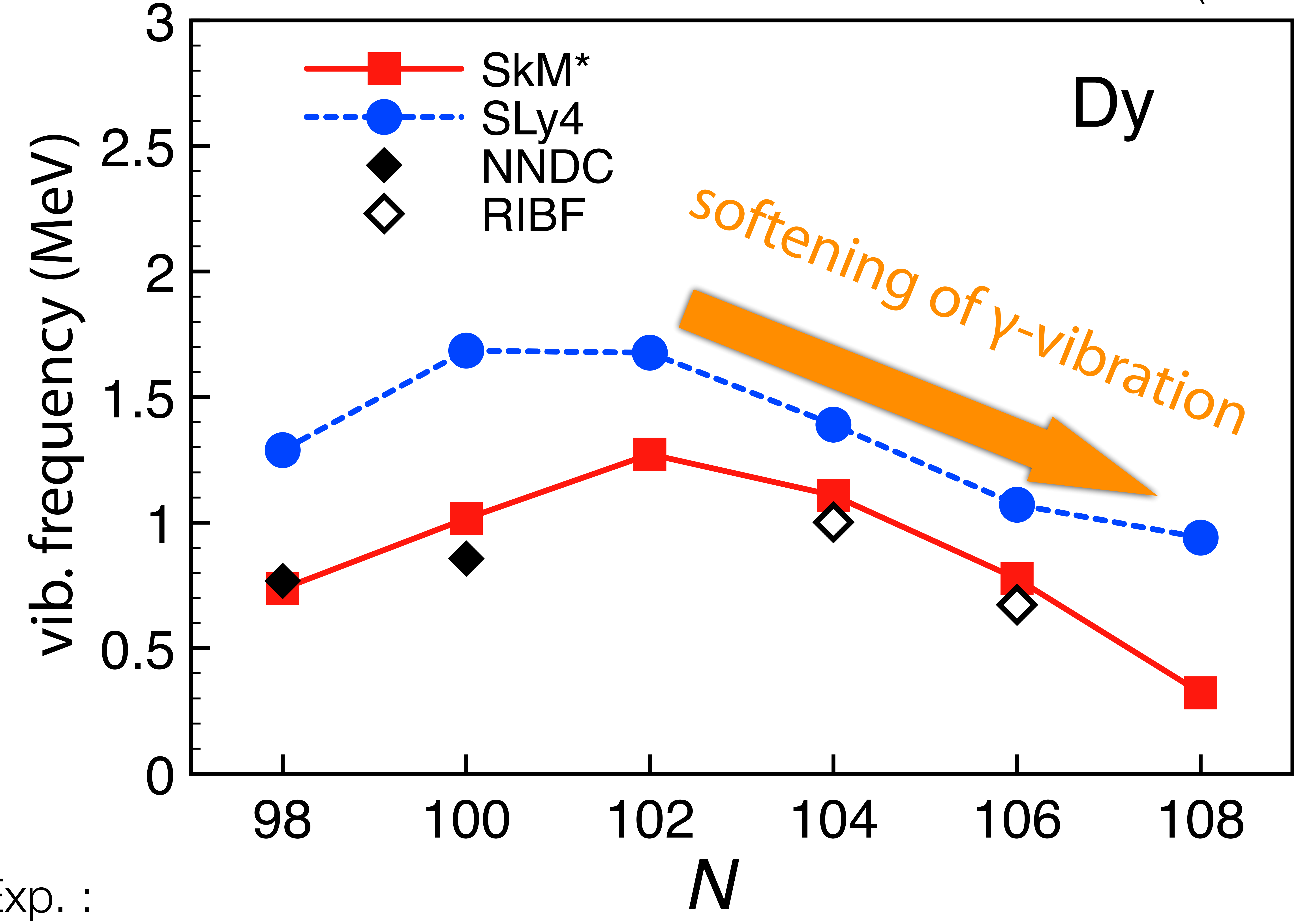

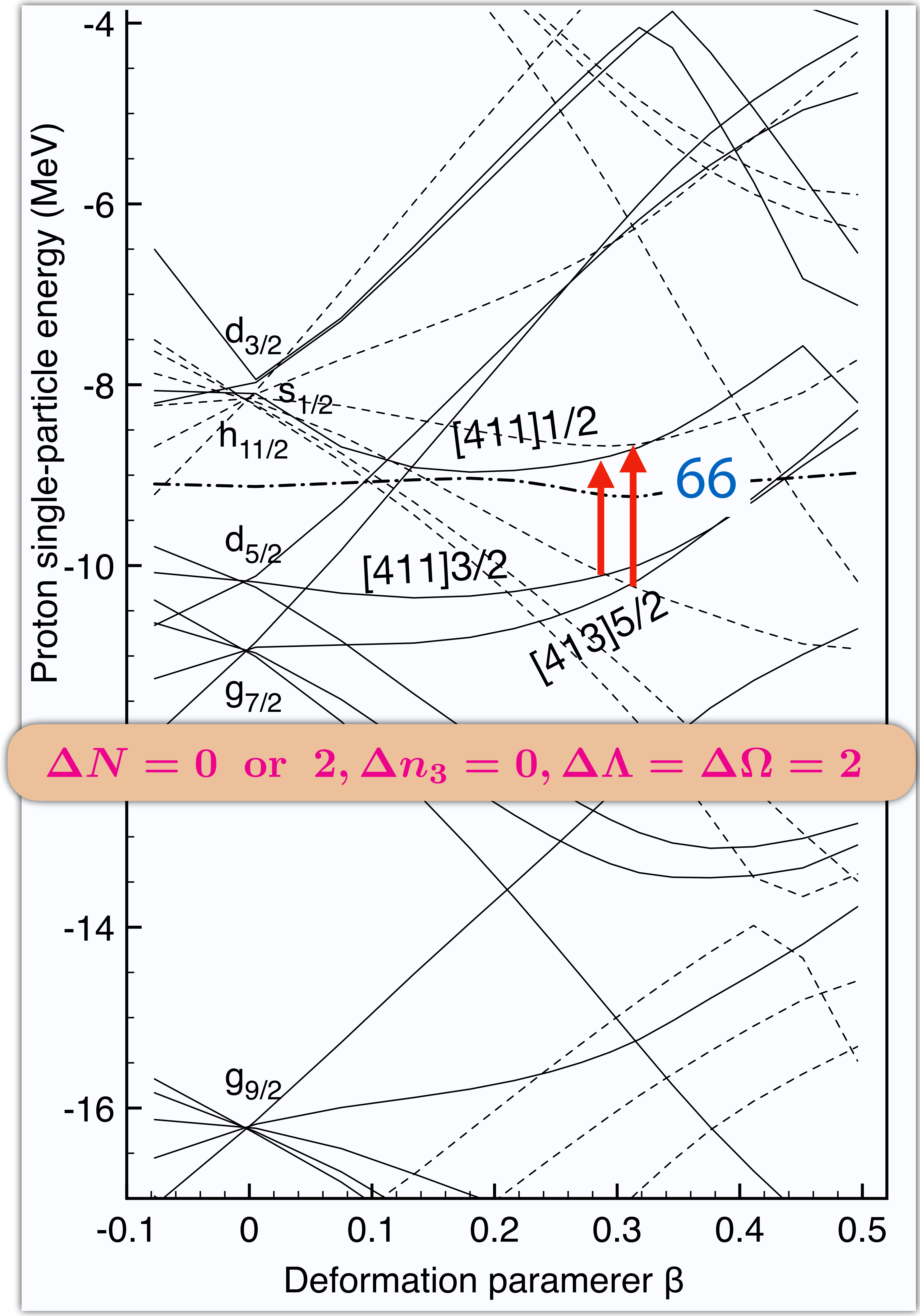

Exp. :

N=104: Söderström+ (2016)

N=106: Watanabe+ (2016)

Gamma vibration in n-rich Dy isotopes

Yoshida–Watanabe (2016)

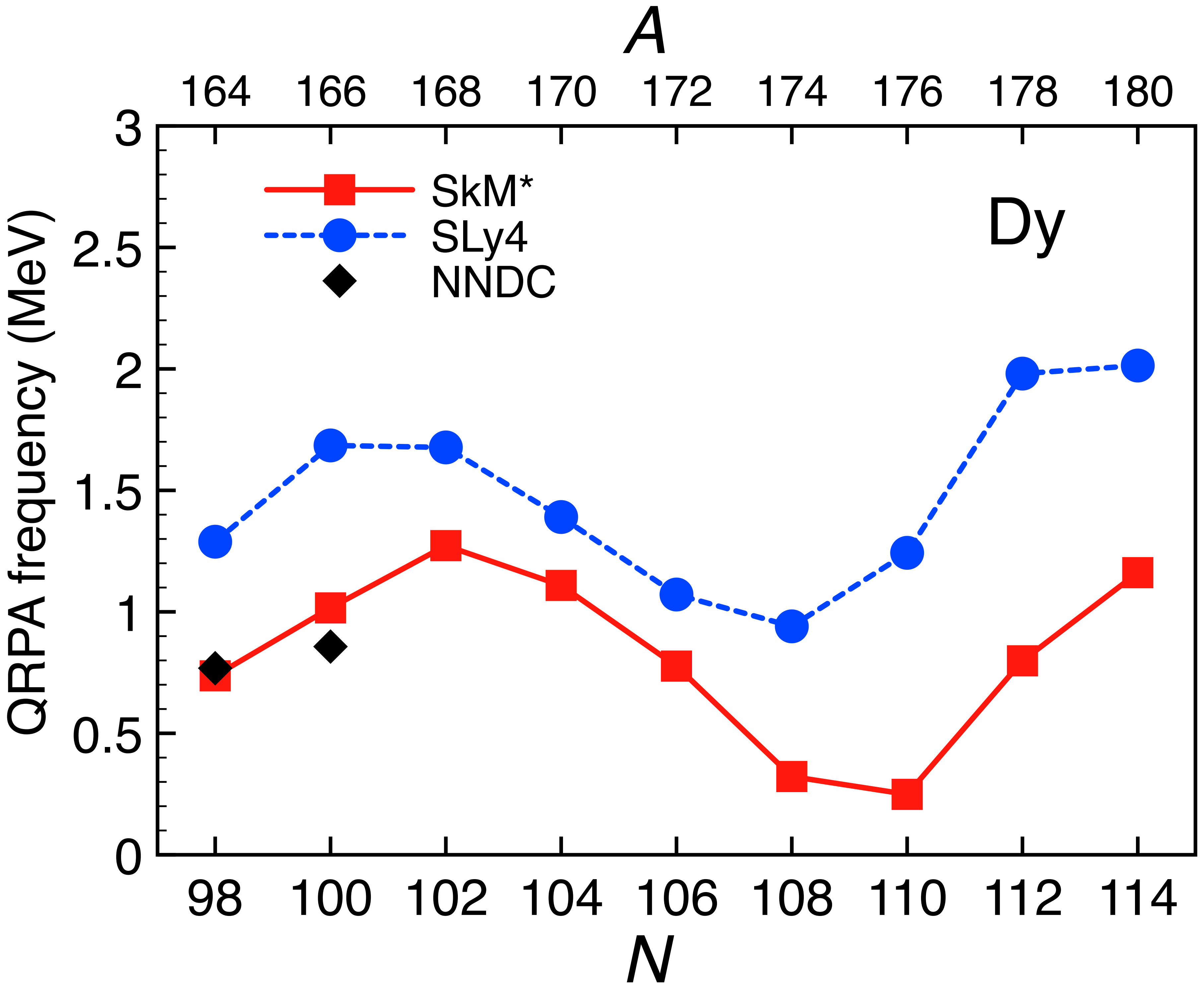

$\Delta N = 0 \text{ or } 2, \Delta n_3 = 0, \Delta\Lambda = \Delta\Omega = 2$

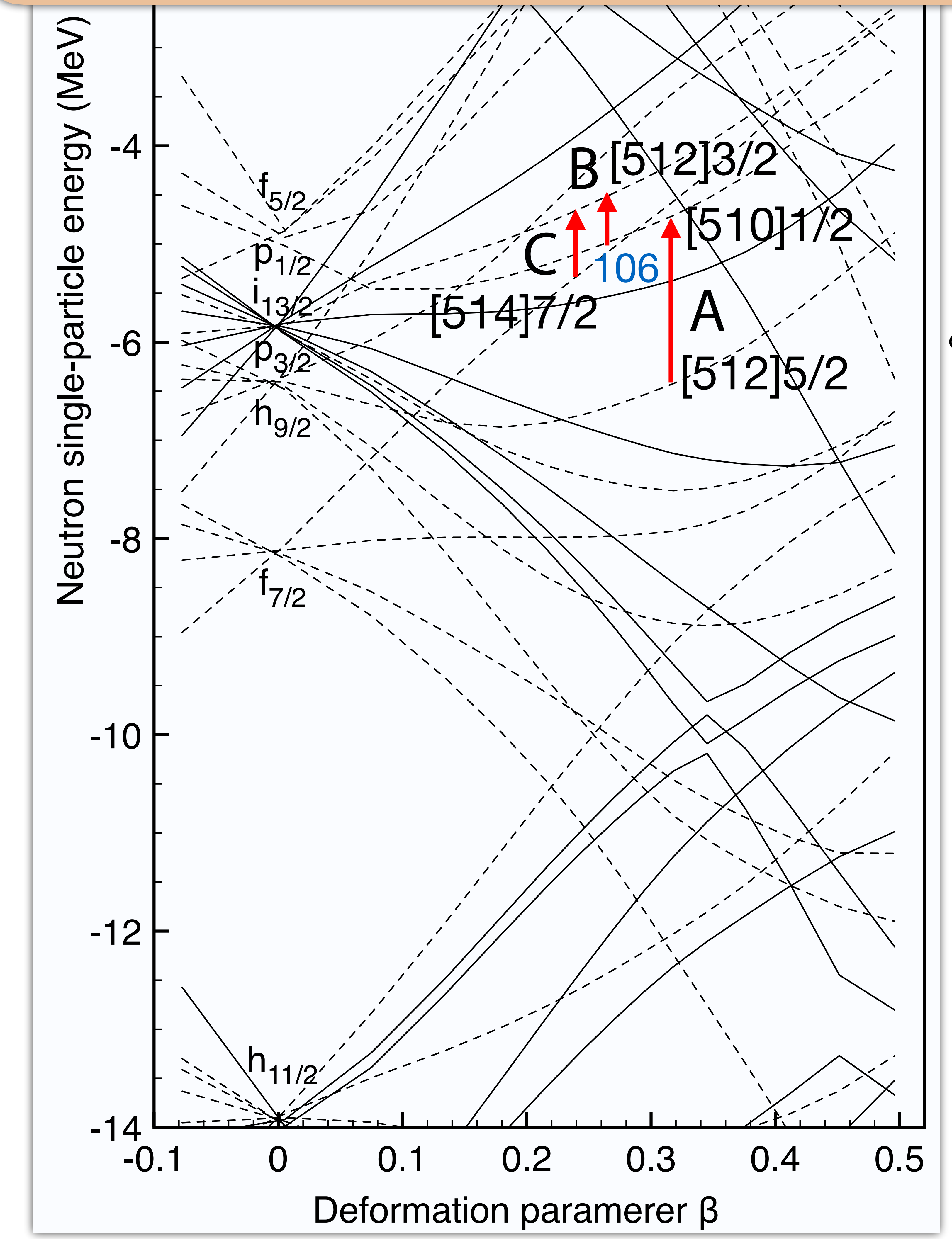

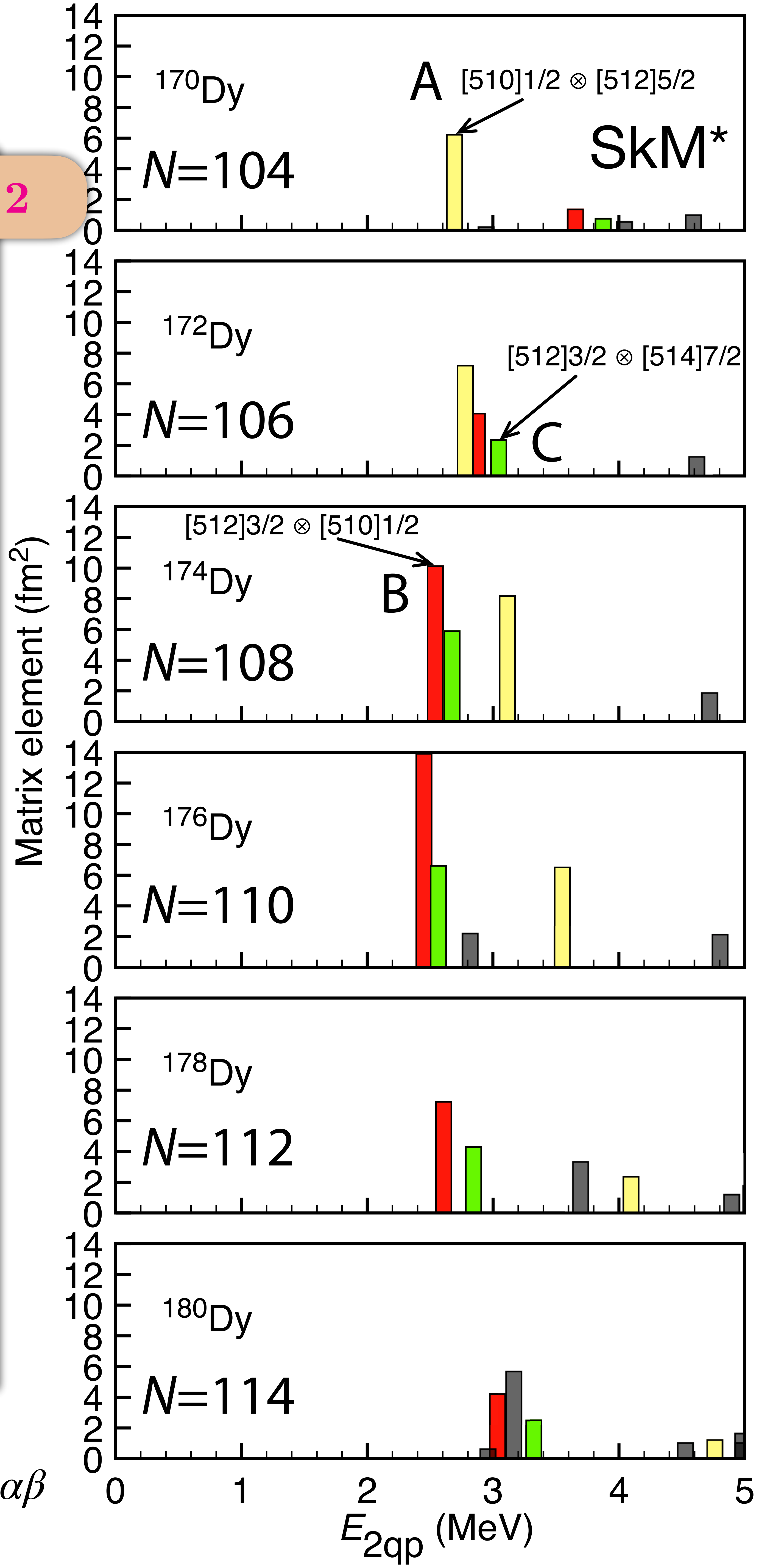

$\omega_{K=2} < 2\Delta$

shell structure

lowest at $N = 108, 110$

$$\langle \lambda | \hat{Q}_{22} | 0 \rangle = \sum_{\alpha\beta} M^{\lambda}_{22,\alpha\beta}$$

IV dipole responses in neutron-rich nuclei

Pygmy Dipole Resonance/Low-Energy Dipole: Many open problems

deepen the understanding of the PDR from a wider perspective

multi-messenger investigation: $(\alpha, \alpha'), (p, p'), (\gamma, \gamma'), (\mathrm{HI}, \mathrm{HI}')$

$+$ **charge-exchange excitation**

$$\hat{F}_{K\mu} = \int d\boldsymbol{r} \sum_{\sigma\sigma'} \sum_{\tau\tau'} r Y_{1K}(\hat{r}) \delta_{\sigma\sigma'} \langle \tau \,|\, \tau_\mu \,|\, \tau' \rangle \hat{\psi}^\dagger(\boldsymbol{r}\sigma\tau) \hat{\psi}(\boldsymbol{r}\sigma'\tau')$$

IV mode: not only $\mu = 0$ but charge-exchange $\mu = \pm 1$

New types of excitation mode in $\mu = \pm 1$?

other than the anti-analog GDR

IV dipole responses: charge-exchange channel

$\mu = -1: (p, n)$ type

SkM*, Γ=2.0 MeV

KY(2017)

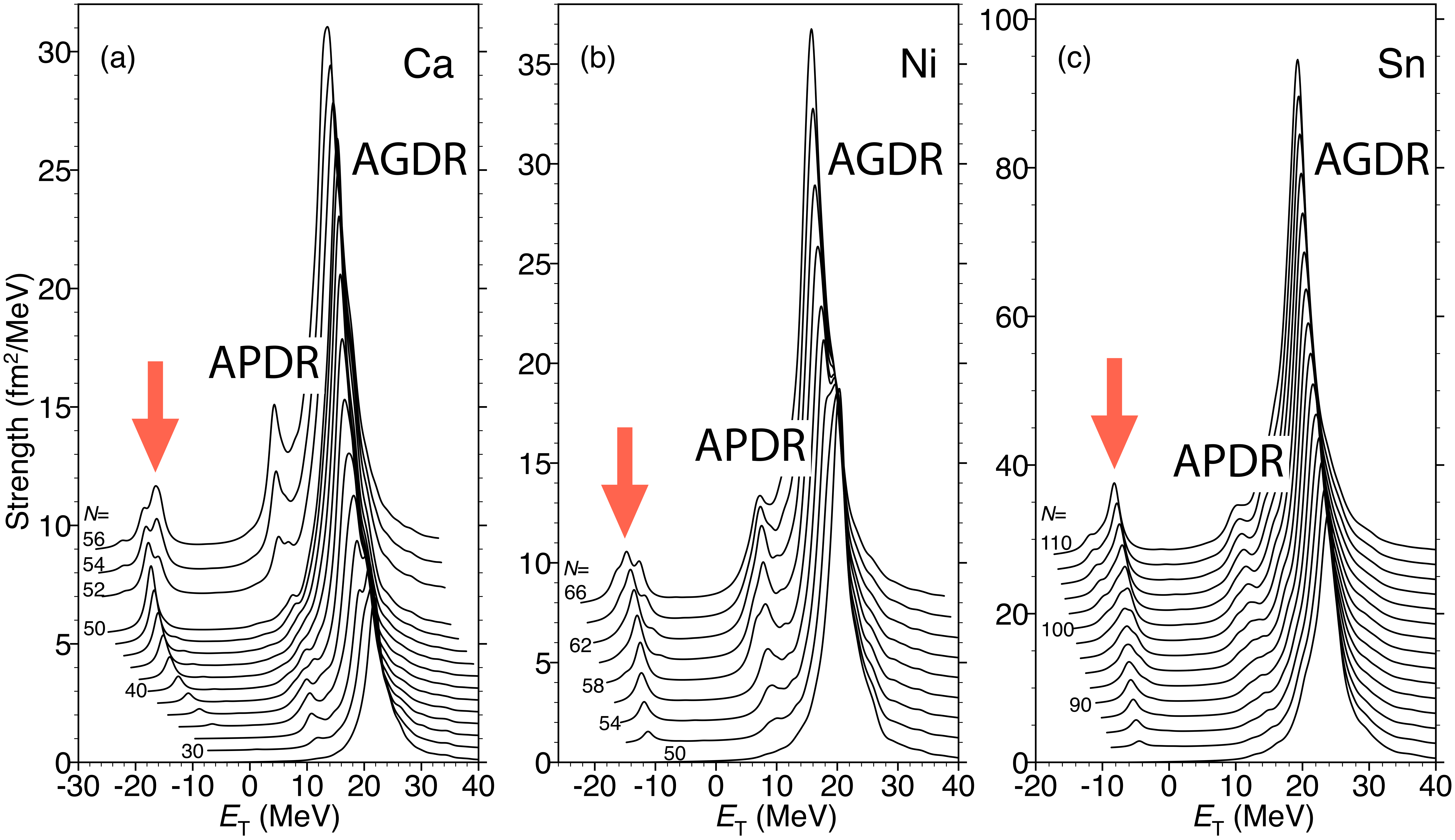

Anti-analog PDR and GDR

transition density

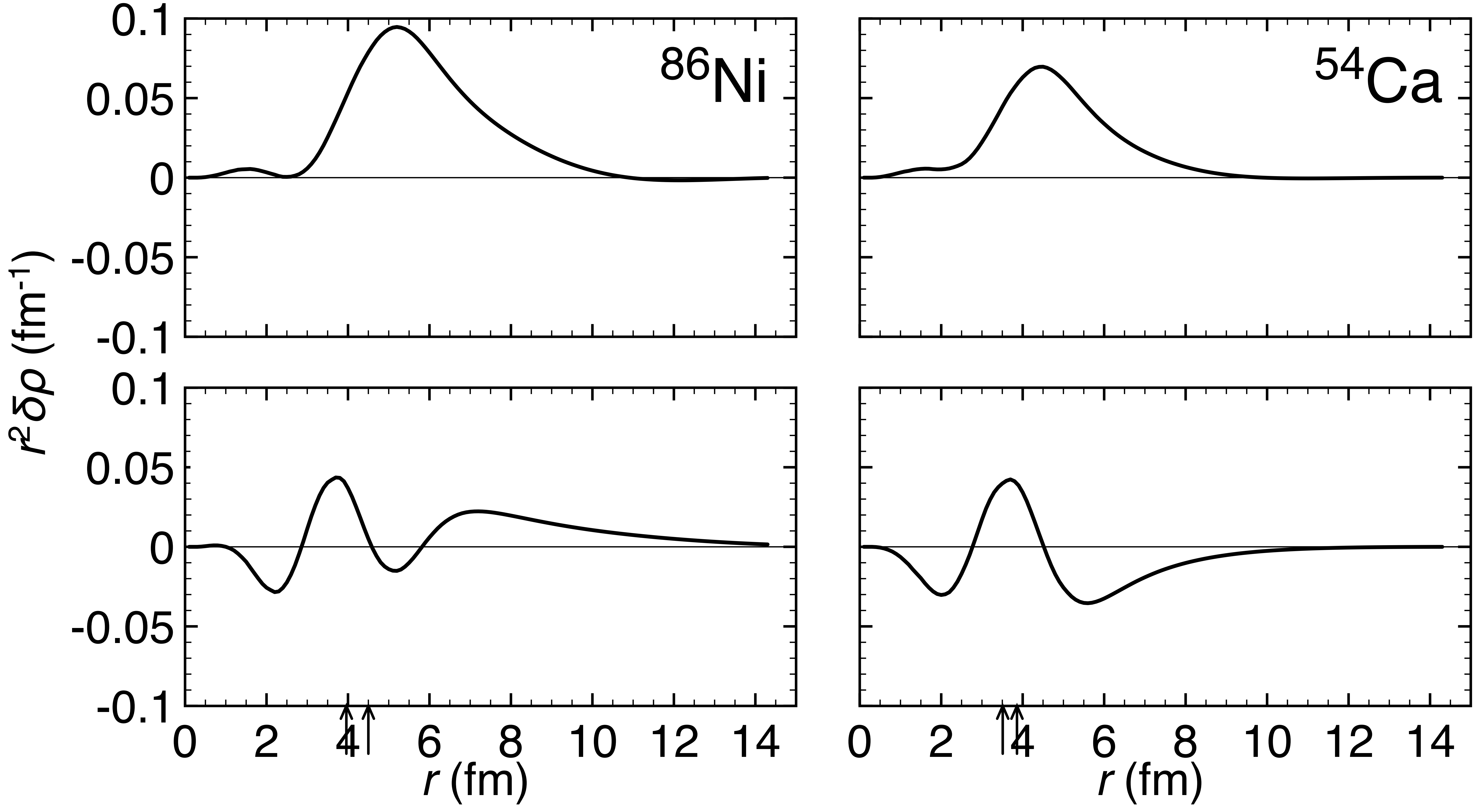

AGDR

pronounced IV character around the surface

APDR

not a simply IV mode

IS/IV mixing

spatially extended structure

weakly-bound neutrons

Cross-shell $-1\hbar\omega_0$ excitation

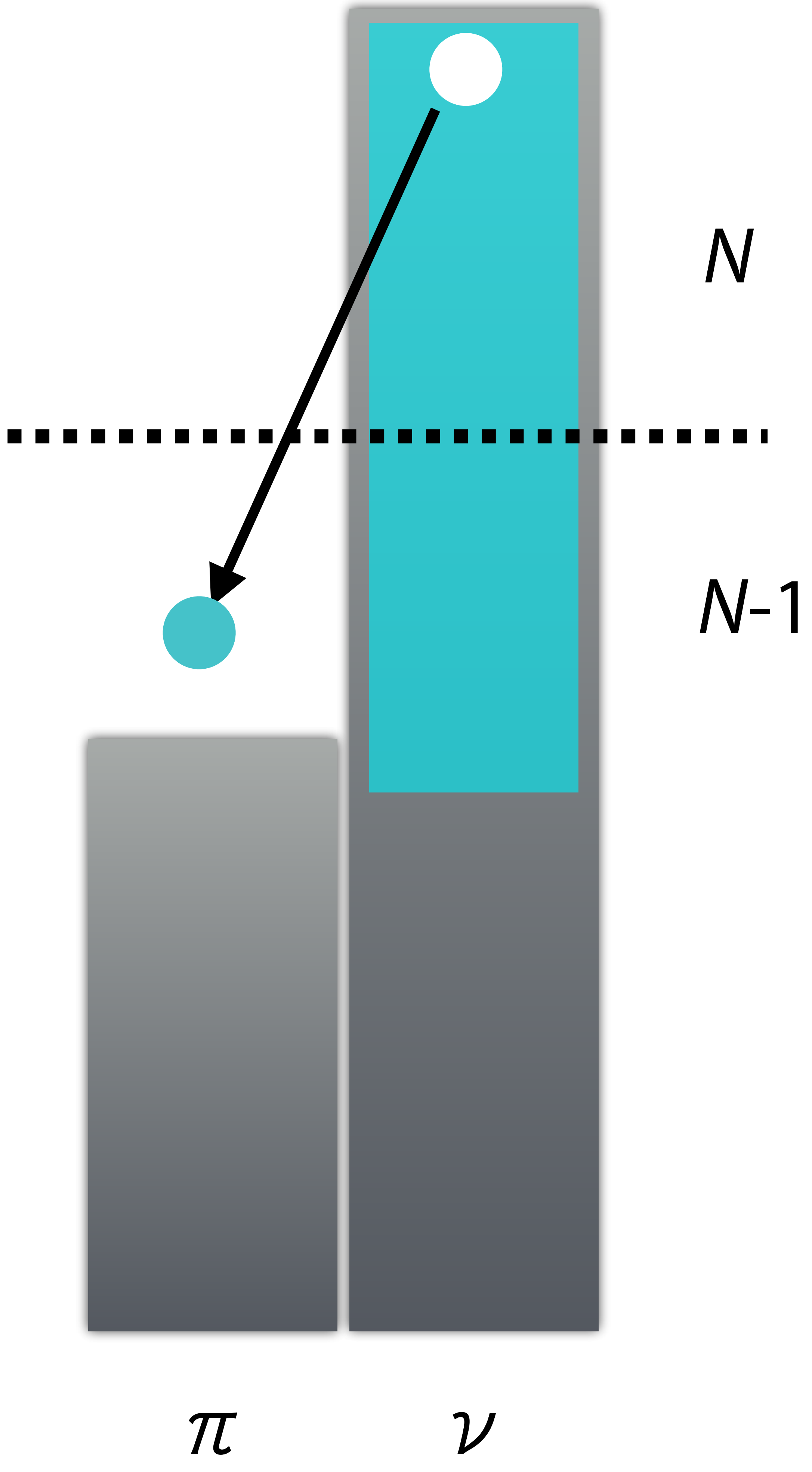

protons are deeply bound

should be distinguished from the anti-analog of PDR

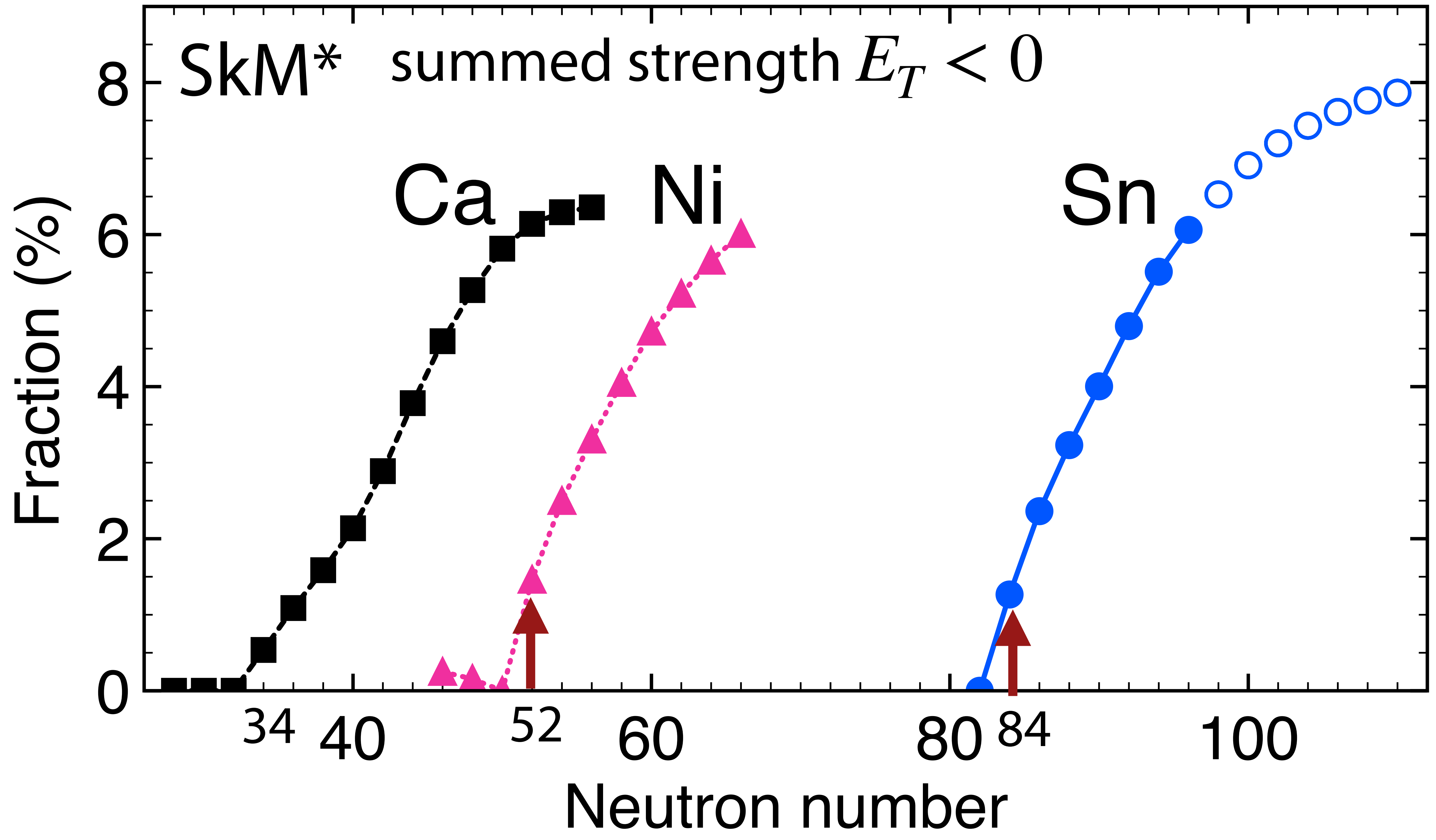

occupation of $2d_{5/2}$ occupation of $2f_{7/2}$

$\nu d_{5/2} \rightarrow \pi p_{3/2}$ $\nu f_{7/2} \rightarrow \pi d_{5/2}$

Cross-shell $-1\hbar\omega_0$ excitation: impact on β-decay rate

allowed transitions only

SkM*

KY(2019)

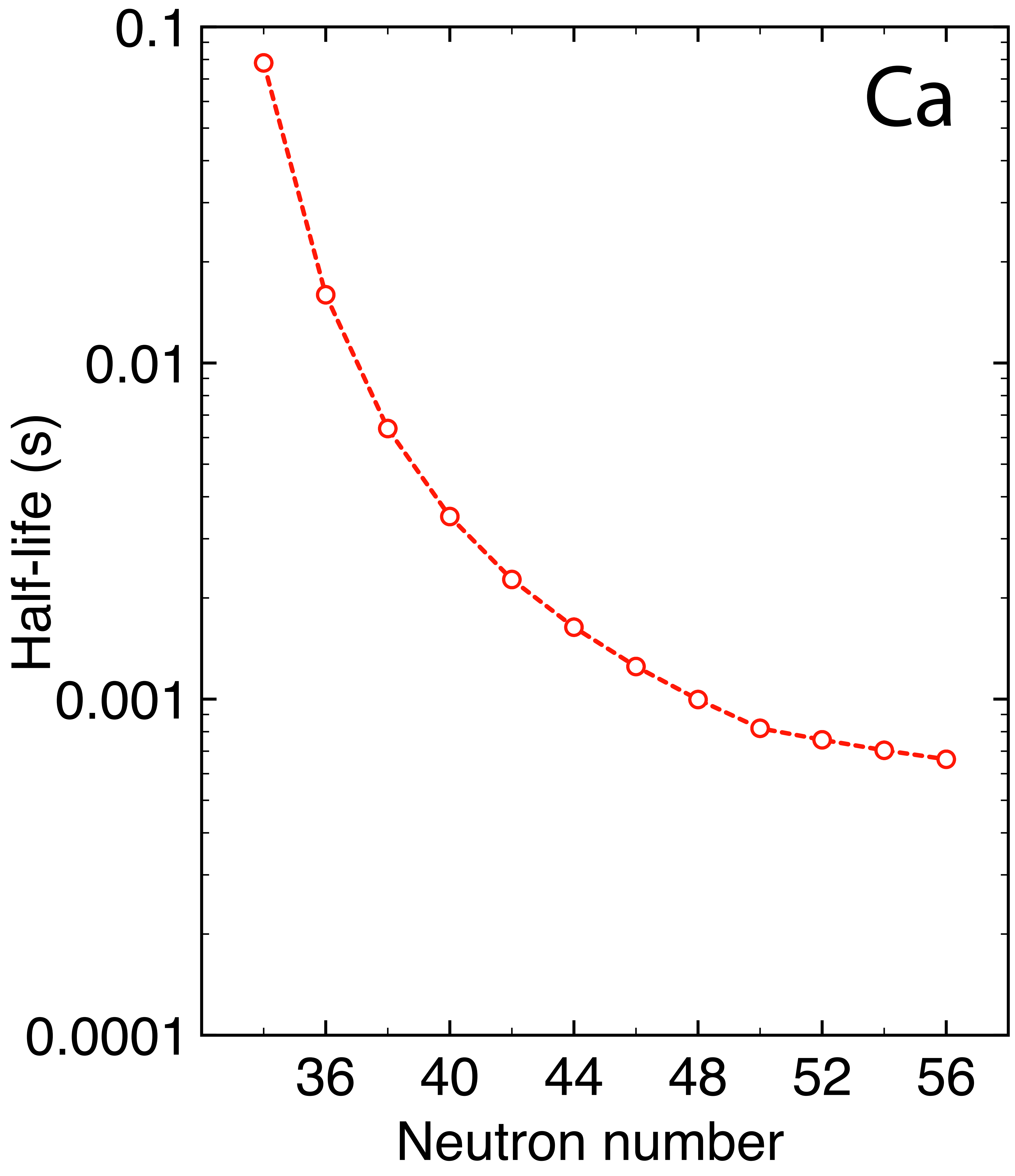

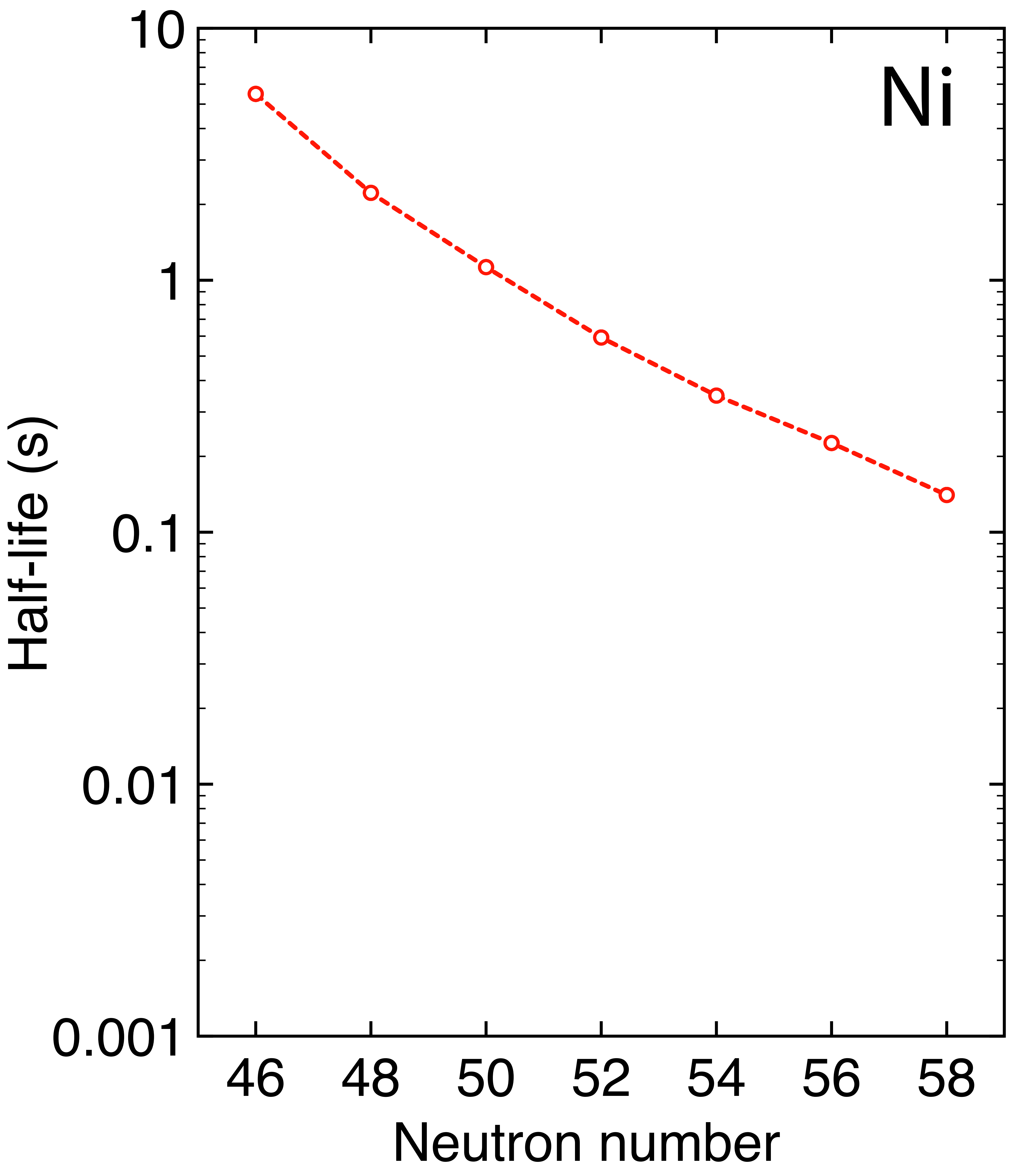

Cross-shell $-1\hbar\omega_0$ excitation: impact on β-decay rate

first-forbidden transitions included

SkM*

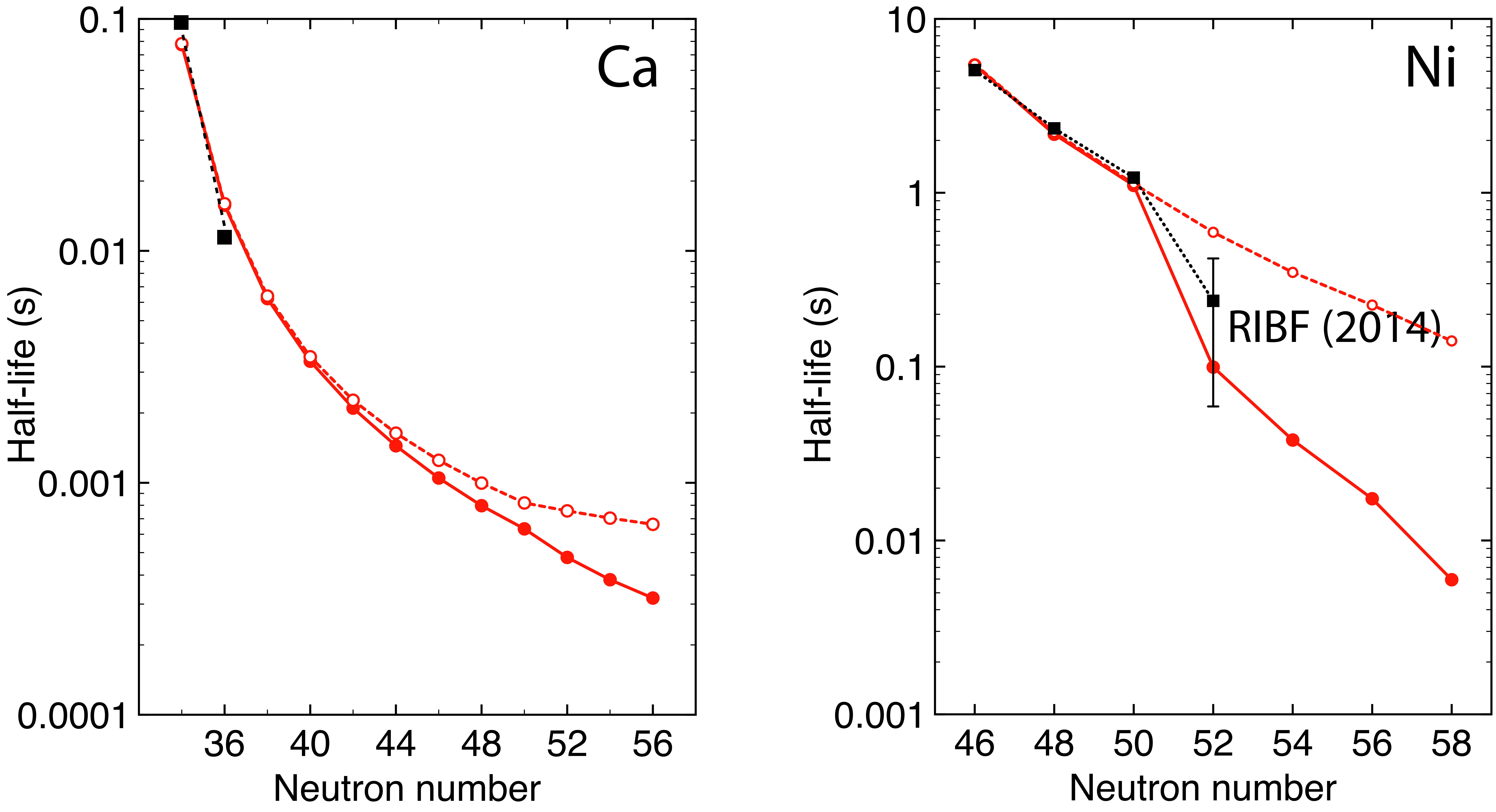

KY(2019)

Summary

Nuclear energy-density functional method in the framework of TDDFT

powerful tool to describe the collective modes in unstable nuclei

coordinate-space representation

high feasibility for systematic calculations thanks to HPC

Rotational mode unique in neutron-rich nuclei

$E(2^+) \leftrightarrow B(E2)$ relation found in stable nuclei can be different due to the isospin-dependence of pairing

Vibrational modes

low-frequency excitations are sensitive to the shell effect and pairing, common in stable nuclei

roles of spatially extended neutrons appear near the drip line

Next

Yrare bands (γ band, octupole band..): interplay between vibration and rotation near the drip line

Triaxially deformed nuclei: β-decay, halo,…

Role of the IV-density dependence

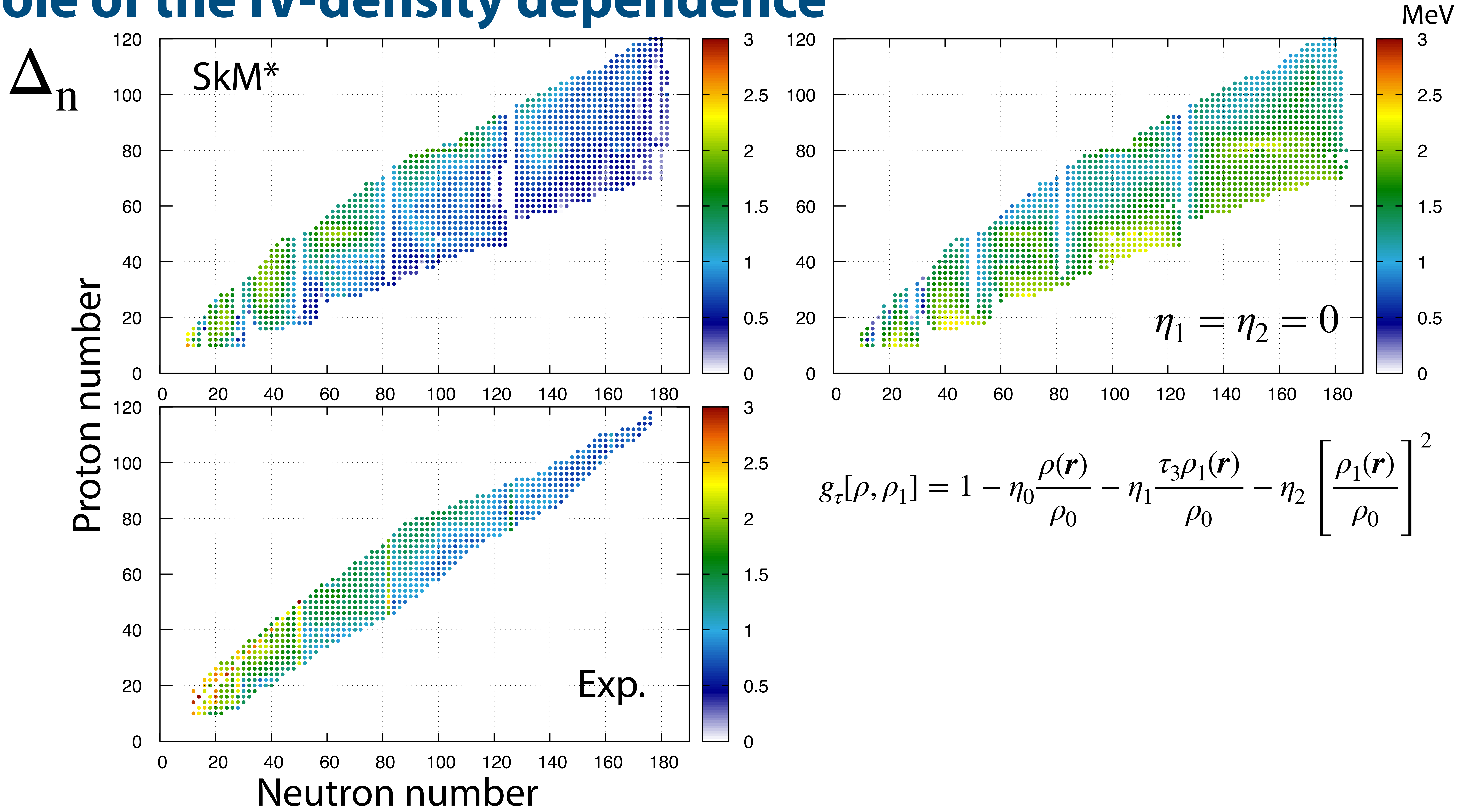

$$g_\tau[\rho, \rho_1] = 1 - \eta_0 \frac{\rho(\boldsymbol{r})}{\rho_0} - \eta_1 \frac{\tau_3 \rho_1(\boldsymbol{r})}{\rho_0} - \eta_2 \left[\frac{\rho_1(\boldsymbol{r})}{\rho_0} \right]^2$$

MoI and the pairing

Q-Value Systematics for Isovector Giant Resonances Excited by (p,n) Reactions on Zr, Nb, Mo, Sn, and Pb Isotopes

W. A. Sterrenburg, Sam M. Austin, R. P. DeVito, and Aaron Galonsky
Cyclotron Laboratory, Michigan State University, East Lansing, Michigan 48824
(Received 7 July 1980)

The (p,n) reaction at 45 MeV is used to study two broad peaks found previously with the target ^{90}Zr. They have now been observed with all but one of seventeen targets from ^{90}Zr to ^{208}Pb. Energy systematics favor the conclusion that these peaks are antianalogs of the giant $M1$ and $E1$ resonances in the target nucleus. The first experimental determinations of T, $T-1$ splittings of the giant $E1$ resonance are reported. Their low values in comparison to T, $T+1$ splittings observed previously can be interpreted as due to a tensor part of the effective isospin potential.

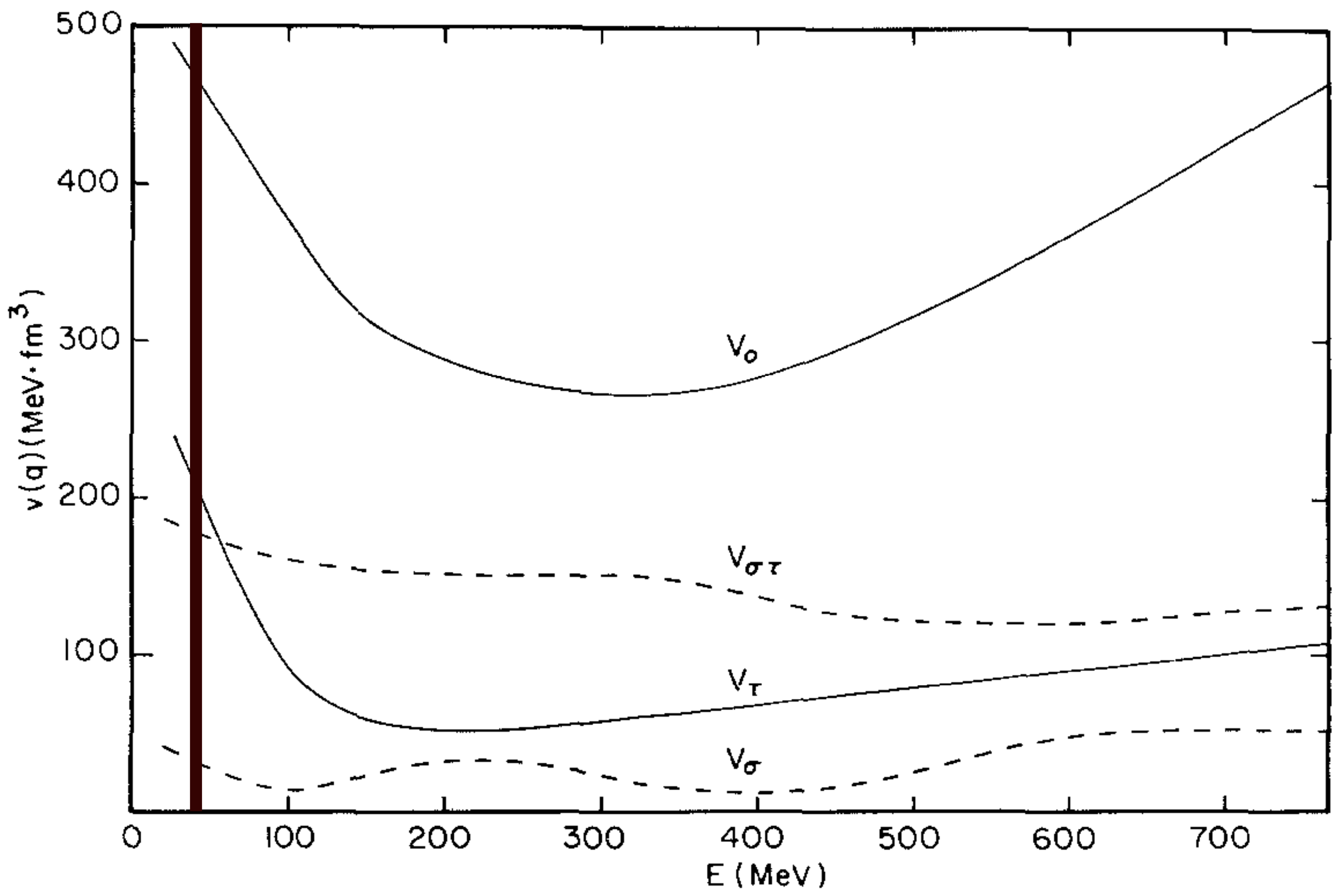

P. Petrovich and W. G. Love, NPA354(1981)499c

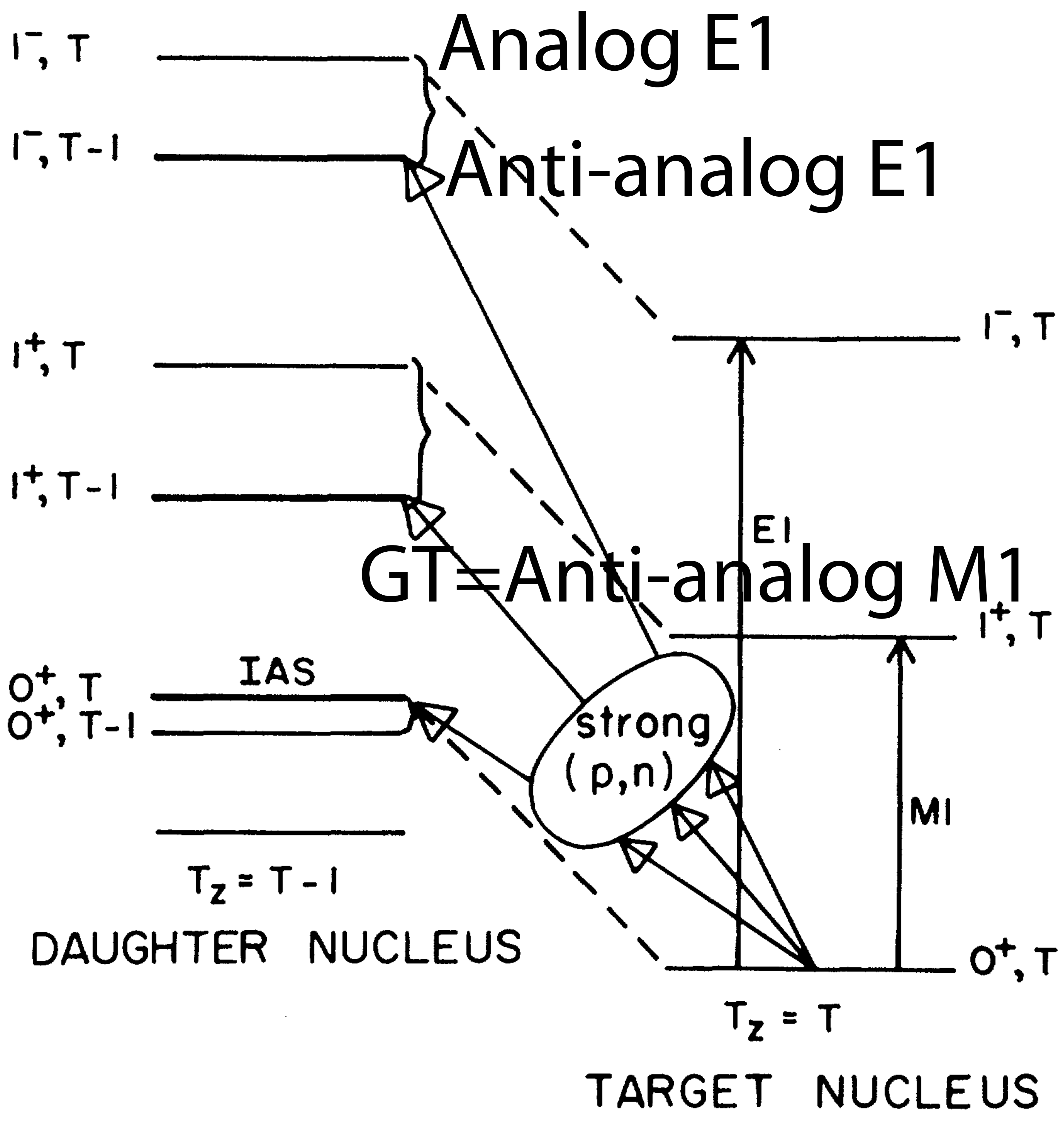

FIG. 1. Some states of the target nucleus ($T_z = T$) and their analogs (isospin $= T$) and antianalogs (isospin $= T-1$) in the $T_z = T-1$ nucleus resulting from a (p,n) reaction. The target states are the ground state and the $M1$ and $E1$ giant resonant states. Isospin geometry strongly favors the three transitions indicated.